



Characterization of late Campanian and Maastrichtian planktonic foraminiferal depth habitats and vital activities based on stable isotopes

Sigal Abramovich^{a,*}, Gerta Keller^a, Doris Stüben^b, Zsolt Berner^b

^a Department of Geosciences, Princeton University, Princeton, NJ 08544, USA

^b Institute für Petrographie und Geochemie, Universität Karlsruhe, Karlsruhe 76128, Germany

Received 31 May 2002; accepted 25 July 2003

Abstract

Depth habitats of 56 late Cretaceous planktonic foraminiferal species from cool and warm climate modes were determined based on stable isotope analyses of deep-sea samples from the equatorial Pacific DSDP Sites 577A and 463, and South Atlantic DSDP Site 525A. The following conclusions can be reached: *Planoglobulina multicamerata* (De Klasz) and *Heterohelix rajagopalani* (Govindan) occupied the deepest plankton habitats, followed by *Abathomphalus mayaroensis* (Bolli), *Globotruncanella havanensis* (Voorwijk), *Gublerina cuvillieri* Kikoine, and *Laeviheterohelix glabrans* (Cushman) also at subthermocline depth. Most keeled globotruncanids, and possibly *Globigerinelliodes* and *Racemiguembelina* species, lived at or within the thermocline layer. *Heterohelix globulosa* (Ehrenberg) and *Rugoglobigerina*, *Pseudotextularia* and *Planoglobulina* occupied the subsurface depth of the mixed layer, and *Pseudoguembelina* species inhabited the surface mixed layer. However, depth ranking of some species varied depending on warm or cool climate modes, and late Campanian or Maastrichtian age. For example, most keeled globotruncanids occupied similar shallow subsurface habitats as *Rugoglobigerina* during the warm late Campanian, but occupied the deeper thermocline layer during cool climatic intervals. Two distinct types of ‘vital effect’ mechanisms reflecting photosymbiosis and respiration effects can be recognized by the exceptional $\delta^{13}\text{C}$ signals of some species. (1) Photosymbiosis is implied by the repetitive pattern of relatively enriched $\delta^{13}\text{C}$ values of *Racemiguembelina* (strongest), *Planoglobulina*, *Rosita* and *Rugoglobigerina* species, *Pseudoguembelina excolata* (weakest). (2) Enriched respiration ^{12}C products are recognized in *A. mayaroensis*, *Gublerina acuta* De Klasz, and *Heterohelix planata* (Cushman). Isotopic trends between samples suggest that photosymbiotic activities varied between localities or during different climate modes, and may have ceased under certain environmental conditions. The appearance of most photosymbiotic species in the late Maastrichtian suggests oligotrophic conditions associated with increased water-mass stratification.

© 2003 Elsevier B.V. All rights reserved.

Keywords: late Cretaceous; planktonic foraminifera; stable isotopes; depth habitats; vital effects

1. Introduction

* Corresponding author. Fax: +1-609-258-1671.

E-mail address: sigala@princeton.edu (S. Abramovich).

Oxygen and carbon stable isotope analyses of

fossil planktonic foraminifera provide information on paleohabitats, paleotemperature and paleofertility. Species ranking based on isotopic signals permits determination of the relative depth stratification within the ocean's upper water masses and traces various biological paleo-activities (e.g. symbiosis, metabolism, nutrition). The accuracy and reliability of these interpretations primarily depend on the quality of the analyzed material (e.g. preservation, diagenesis), recognition of the effects of species biological activities (e.g. vital effects), and effects of environmental variability upon isotopic signals. In contrast, species population abundance data quantify a species response to the environmental changes recorded in stable isotope data. The combination of stable isotope and quantitative species analysis thus provides a powerful tool for paleoecological and paleoclimatic studies, particularly of the late Cretaceous (for a summary, see Keller, 2001).

During the late Cretaceous planktonic foraminifera experienced the highest morphological and taxonomic diversity in their evolutionary history (Masters, 1977; Li and Keller, 1998a). A major increase in species diversification began in the late Campanian and reached a maximum (>60 species) during the early Maastrichtian (Li and Keller, 1998a, 1999). This trend corresponds to the onset of a global cooling that began at about 73 Ma (late Campanian) and ended the Cretaceous greenhouse climate mode. The congruency between plankton diversification and climate cooling probably signifies the presence of new potential niches for planktonic foraminifera in the upper water column.

The onset of cooling in the late Campanian and its progression into the early Maastrichtian is recorded at various deep-sea localities (see summary by Barrera and Savin, 1999). $\delta^{18}\text{O}$ records of single benthic and planktonic foraminiferal species at South Atlantic DSDP Site 525A indicate a major temperature drop (5–6°, 4–5°, respectively) between ~ 73 and 70 Ma (Li and Keller, 1998a, Fig. 1). A similar trend is recorded at the equatorial Pacific DSDP Site 463 by benthic foraminifera, though surface (planktonic foraminifera) $\delta^{18}\text{O}$ records do not indicate a decrease in temperatures (Li and Keller, 1999, Fig. 2). Between 70

and 68.5 Ma temperatures temporarily warmed. Thereafter cooling resumed and persisted until $\sim 500\,000$ years before the K–T boundary when water temperatures reached maximum cooling for the Maastrichtian (Li and Keller, 1998b, Fig. 1). Between 450 000 and 200 000 years preceding the K–T boundary, global climate warmed rapidly, raising both sea surface and intermediate water temperatures by as much as 3–4°C. Climate cooling accelerated during the final 100 000 kyr of the Maastrichtian (Li and Keller, 1998a,b, Fig. 1).

Planktonic foraminiferal populations were directly affected by these extreme climatic oscillations. Throughout the late Maastrichtian species diversification almost ceased and species extinctions exceeded evolution (Abramovich et al., 1998; Li and Keller, 1998a,c). At the Cretaceous–Tertiary boundary (K–T boundary) the Cretaceous planktonic foraminiferal epoch came to an end with the majority of species (e.g. all tropical and subtropical species) becoming extinct and only ecological generalist species surviving into the Danian (summaries in Keller, 1996; Keller et al., 2002).

Few studies have examined stable isotopes of late Cretaceous planktonic foraminifera in order to determine their living habitats and ecological preferences (e.g. Douglas and Savin, 1978; Boersma and Shackleton, 1981; D'Hondt and Arthur, 1995). The pioneer study by Douglas and Savin (1978) provided $\delta^{18}\text{O}$ and $\delta^{13}\text{C}$ data on 11 late Campanian and Maastrichtian species from the Pacific (DSDP Sites 47 and 48) and Atlantic (Lamont–Doherty RC5-12) oceans. Subsequently, Boersma and Shackleton (1981) estimated the depth stratification of 25 late Campanian and Maastrichtian species based on $\delta^{18}\text{O}$ data from the Atlantic (DSDP Sites 356 and 384) and Pacific oceans (DSDP Sites 463 and 465A). More recently, D'Hondt and Arthur (1995) analyzed the stable isotope composition of 39 planktonic foraminiferal species from the latest Maastrichtian in three Atlantic deep-sea cores (DSDP Sites 390A and 20C; ODP Site 690C), and Barrera and Keller (1990, 1994) analyzed select species from DSDP Site 738 and Brazos River, Texas. D'Hondt and Zachos (1998), Houston and Huber (1998) and Houston et al. (1999) investigated

Table 1

Location, paleodepths and paleolatitudes of DSDP localities used in this study

	DSDP Site 463	DSDP Site 577A	DSDP Site 525A
Location	Mid-Pacific mountains	Shatsky Rise	Walvis Ridge
Latitude	21°21'N	32°26'N	29°04'S
Longitude	174°40'E	157°43'E	02°59'E
Paleolatitude	~5°S	10°N	36°S
Paleodepth	~1500 m	1500–2000 m	1000–1500 m
References	Boersma (1981); Li and Keller (1999)	Zachos et al. (1985)	Chave (1984); Li and Keller (1998a)

photosymbiotic activities of late Cretaceous species.

The main objective of this study is to examine the habitat patterns and ecological characteristics of late Cretaceous planktonic foraminiferal species based on oxygen and carbon isotope signals of well-preserved foraminiferal tests from deep-sea carbonates. Specific objectives include: (1) establishing a stable isotopic database for most late Campanian and Maastrichtian planktonic foraminiferal species from low and middle latitudes; (2) determining the depth stratification of species within the water column based on the relative isotopic ranking of species; (3) identifying characteristics of specific biological activities of species (e.g. symbiosis, metabolism); and (4) reconstructing changes in species depth stratification and biological activities in different oceanic realms (tropical Pacific, middle Atlantic), and for differ-

ent climate modes (warm and cool late Cretaceous).

2. Materials and methods

2.1. Locations and sample intervals

A total of 12 late Campanian and Maastrichtian time intervals were chosen for this study from three deep-sea localities in the equatorial Pacific (DSDP Sites 577A and 463) and South Atlantic (DSDP Site 525A), at paleolatitudes 10°N, 5°S and 36°S, respectively (Fig. 3; Table 1). From each locality, specific time horizons were selected spanning warm and cool climatic intervals between 74.3 and 65.1 Ma (Tables 1 and 2; Li and Keller, 1998a,b, 1999). Age determination is based on the high-resolution planktonic forami-

Table 2

Estimated ages and planktonic foraminiferal biostratigraphy of sample intervals used in this study

DSDP Sites	Equatorial Pacific	Sample interval	Depth	Stage	Climatic mode	Age	Calcareous foraminiferal zones
		(cm)	(mbsf)			(Ma)	
Site 463	Equatorial Pacific	10-6, 97–100	80.49	Early Maastrichtian	warm	69.3	CF6
		13-3, 97–99	104.48		cool	70.3	CF7
		16-6, 101–103	137.52	Latest Campanian	warm	71.5	CF8a
		20-1, 100–102	168.01	Late Campanian	warmest	72.9	CF9
		21-5, 64–66	183.15			74.3	CF10
Site 577A		13-6, 42–44	122.42	Late Maastrichtian	coldest	68.3–67.74	CF4
		13cc, 18–21	123.2			68.3–67.74	CF4
Site 525A	South Atlantic	40-2, 104–106	452.63	Latest Maastrichtian	coldest	65.1	CF2-1 interval
		40-5, 90–92	457.01	Late Maastrichtian		65.6	top CF3
		41-6, 89–91	468.01			66.8	CF3-4 transition
		48.3, 100–102	530.1	Latest Campanian	warmest	71.5	CF8a
		50-1, 100–102	546.1	Late Campanian		72.3	CF8a

For information on calibration of zones to paleomagnetic record and climatic modes see Figs. 1 and 2.

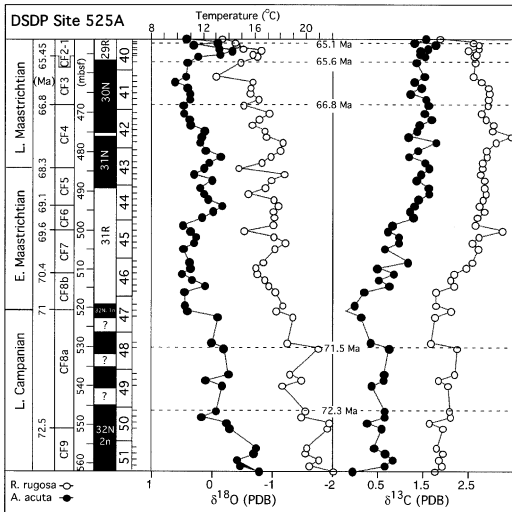


Fig. 1. Biostratigraphy, magnetostratigraphy, paleotemperature, and stable isotope records of planktonic (*Rugoglobigerina rugosa*) and benthic foraminifera (*Cibicidoides pseudoacutus*) of the late Campanian–Maastrichtian at DSDP Site 525A (data from Li and Keller, 1998a). The estimated ages of the five selected sample intervals correspond to the relatively warm late Campanian (72.3, 71.5 Ma), and coldest late Maastrichtian (66.8, 65.6, 65 Ma) climate intervals. Note the overall increase in $\delta^{13}\text{C}$ between ~ 70.5 and ~ 65.6 Ma, and the rapid decrease thereafter.

niferal zonal scheme (CF zones) developed by Li and Keller (1998a,b, 1999) and calibrated to the paleomagnetic record of Site 525A (Figs. 1 and 2; Table 2). Absolute age estimates for samples are based on average sedimentation rates within each CF biozone and/or magnetostratigraphic (Table 2). Five samples chosen from Site 463 represent the warm and cooler time intervals of the late Campanian and early Maastrichtian (Table 2; Fig. 2). The coldest late Maastrichtian period is missing at Site 463, but was sampled in two intervals at the nearby Site 577A (Fig. 4). Two late Campanian and three late Maastrichtian time intervals were selected at Site 525A, representing the warmest and coldest periods, respectively (Table 2; Fig. 1).

2.2. Sample preparation and specimen selection

From each selected time horizon approximately 20 cm³ of sediment was disaggregated in tap water, ultrasonically cleaned for 15–20 s, washed

over a > 63-µm sieve, and oven-dried at 50°C. Planktonic foraminiferal species were identified (Plates I–V) based on Smith and Pessagno (1983), Robaszynski et al. (1983–1984), Caron (1985) and Nederbragt (1991). Planktonic foraminiferal preservation is very good in the equatorial Pacific DSDP Sites 577A and 463, and good in the South Atlantic DSDP Site 525A (Plate I). Test infillings are rare (< 1%) at the equatorial Pacific sites, but more common (~ 5%) at Site 525A. Test surfaces (external and internal) are clean, but show evidence of secondary recrystallization and minor calcite overgrowth under the scanning electron microscope (Plate I). In addition, fragmented shells (~ 5%) in the washed sample residues suggest some dissolution effects.

For each sample about 10–15 adult specimens were picked from the > 250-µm, and 30–40 adult specimens from the 150–250-µm size fractions for stable isotope analysis. For species with adult specimens in both size fractions, samples were standardized by picking only the larger > 250-µm size fraction. Intraspecies morphologic vari-

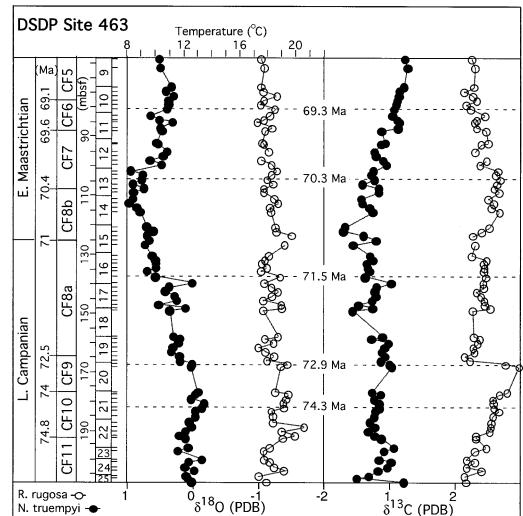


Fig. 2. Biostratigraphy, paleotemperature, and stable isotope records of planktonic (*Rugoglobigerina rugosa*) and benthic foraminifera (*Nuttalides truempyi*) of the late Campanian–early Maastrichtian at DSDP Site 463 (data from Li and Keller, 1998). Estimated ages of the five selected sample intervals correspond to warm climatic intervals in the late Campanian (72.4, 71.5 Ma) and early Maastrichtian (69.3 Ma), and to the relatively cool climate at 70.3 Ma.

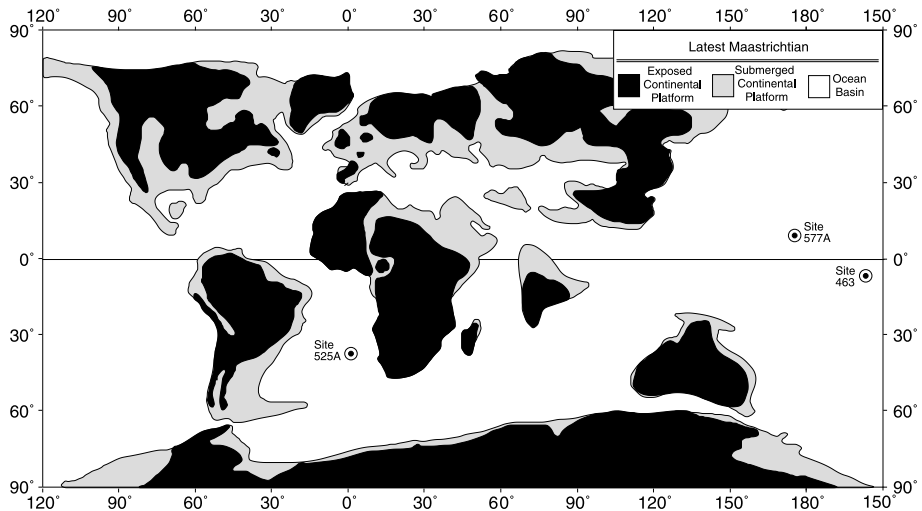


Fig. 3. Maastrichtian paleolocations of DSDP sites used in this study: equatorial Pacific, Sites 463 and 577A, and South Atlantic, Site 525A. Modified from Li and Keller (1999).

ability, ontogenetic, physiological and behavioral effects (e.g. depth migration, incorporation of respiration CO₂ during calcification; Emiliani, 1971; Lohmann, 1995; Spero and Lea, 1996) were limited by choosing only adult morphologies, particularly for *Pseudotextularia elegans* (Rzehak) (wide apertures), *Planoglobulina carseyae* (Plummer) (terminal multiserial chambers), *Heterohelix glo-*

bulosa (not including *H. striata*) (Ehrenberg) ([Plates II and IV](#)). To reduce the effects of dissolution and secondary recrystallization on the stable isotope values, only individuals were chosen with: (1) complete (unbroken) tests, (2) without chamber infilling, (3) clean external test surfaces, and (4) none or only minor calcite overgrowth on tests. Examinations of secondary recrystallization of planktonic foraminiferal wall structures were performed with a light microscope and a scanning electron microscope (Philips XL30 FEG-SEM) at Princeton University ([Plate I](#)).

2.3. Species analysis

Stable isotope analyses of species were conducted on multiple sample intervals to evaluate the isotopic ordering and intraspecies variability between sample intervals. The number of measurements performed for each species range between 1 and 12 and depends primarily on the species evolutionary range, biogeographic limits, abundance and preservation state in each sample interval ([Appendix 1](#)). A larger number of species were analyzed from the equatorial Pacific (DSDP Sites 577A and 463) than from the South Atlantic (DSDP Site 525A), due to higher species richness in lower latitudes. For example, the coldest late Maastrichtian time intervals at Site 577A yielded

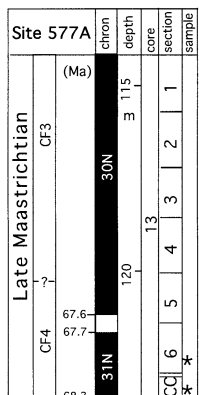
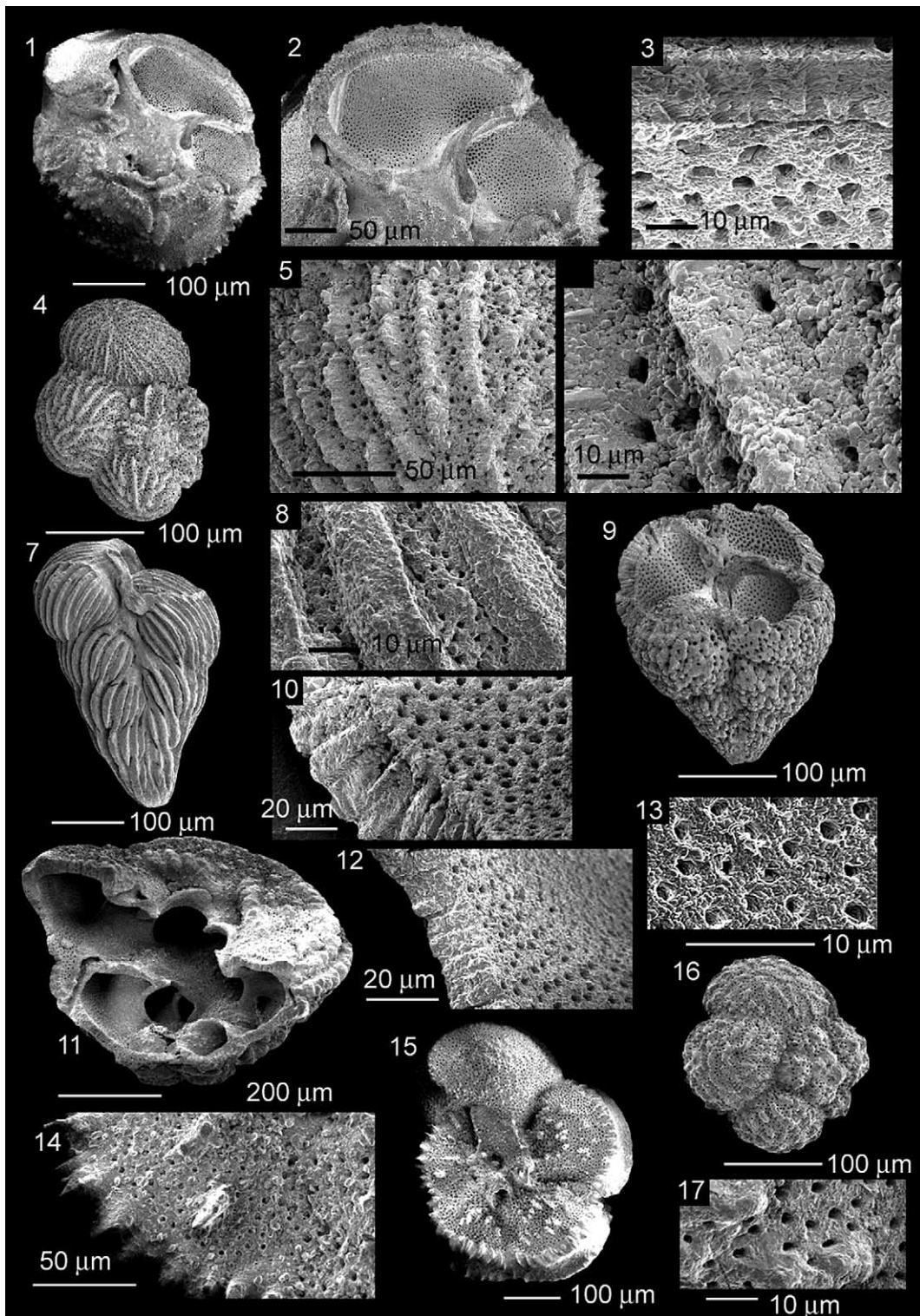


Fig. 4. Estimated age range between 68.3 and 67.7 Ma of the two sample intervals selected from core 13 at Site 577A (marked by asterisk). Maximum age defined by the top of Chron 31N. Minimum age defined by the base of the planktonic foraminiferal Zone CF4 (first appearance of *Racemiciguembelina fructicosa*). Paleomagnetic data from Bleil (1985), magnetochron ages from Berggren et al. (1995) and CF zones from Li and Keller (1998a).



40 species, compared to 28 species from the corresponding time interval at Site 525A. Similarly, 30 species were measured from the late Campanian–early Maastrichtian time intervals at Site 463, compared with 15 from the late Campanian at Site 525A (Appendix 1). Species were classified by depth habitat or biological activities (Sections 4.2 and 4.3; Table 3) based primarily on consistency in relative isotopic ordering ($\delta^{13}\text{C}$ and $\delta^{18}\text{O}$) in the various time horizons, rather than absolute values. The rational is that variations in the absolute isotopic values of species mostly reflect environmental differences and the degree of diagenetic overprinting between samples, whereas relative isotopic ordering reflects habitat distribution and is less affected by these factors.

2.4. Stable isotopes

Stable isotope analyses were carried out by means of an automated carbonate preparation system (MultiCarb) connected on-line to an isotope ratio mass spectrometer (Optima, from Micromass UK Ltd.). Accuracy was checked in each of the analytical batches by running the carbonate standard NBS-19. External precision is $\pm 0.05\text{\textperthousand}$ for carbon isotopes and $\pm 0.08\text{\textperthousand}$ for oxygen isotopes. Isotope values are reported in the δ -notation relative to the Vienna-PDB standard for both carbon and oxygen (Appendix 1). Paleotemperature estimates were calculated using the equation of Erez and Luz (1983), with seawater $\delta^{18}\text{O} =$

$-1.2\text{\textperthousand}$ corresponding to continental ice free world (Shackleton and Kennett, 1975).

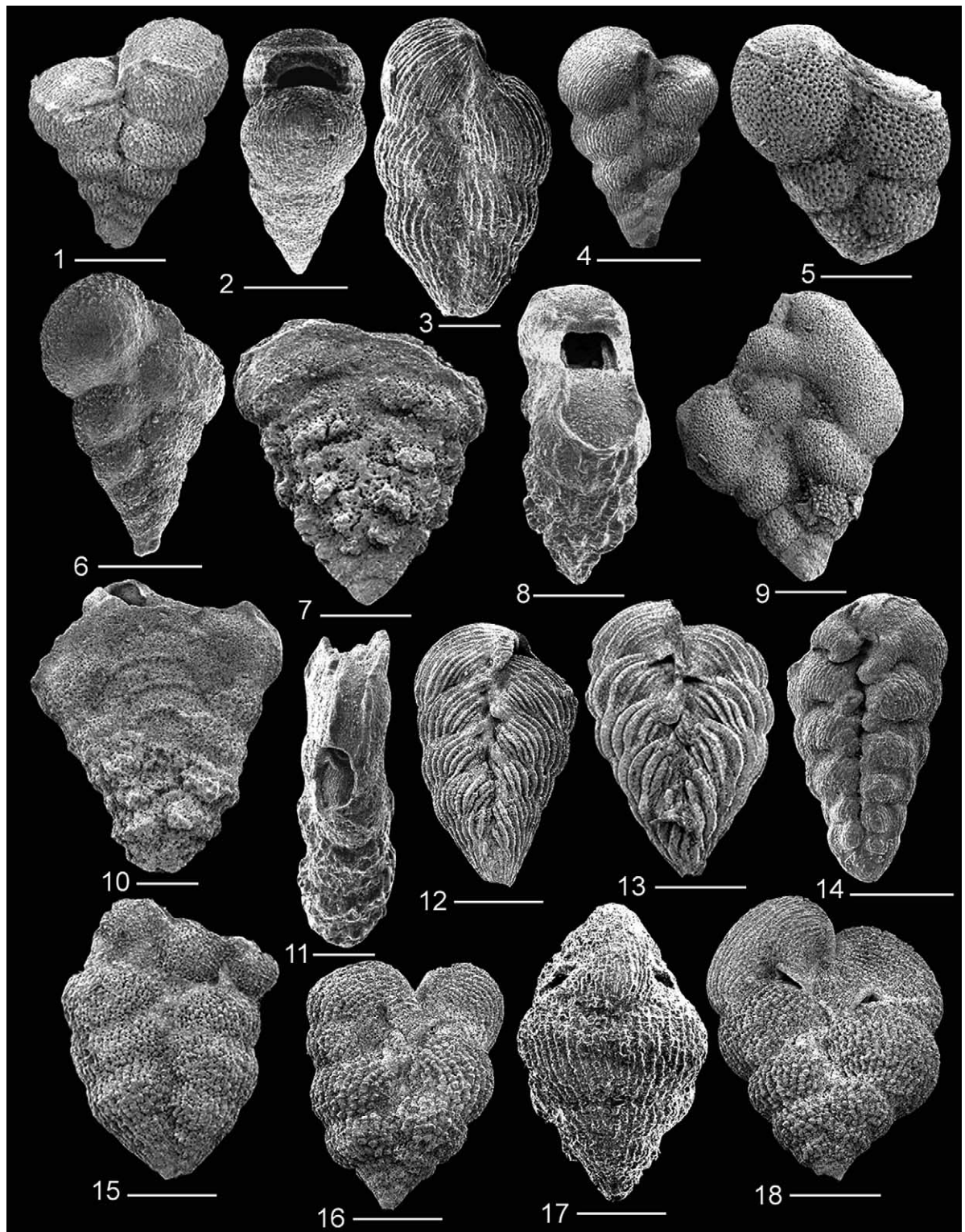
3. Results

3.1. Late Cretaceous $\delta^{18}\text{O}$ trends

The relatively warm late Campanian climate mode described by Barrera (1994), Li and Keller (1998a, 1999, figs. 2 and 3), and Barrera and Savin (1999) is also reflected in the $\delta^{18}\text{O}$ records of the selected sample intervals from equatorial Pacific DSDP Site 463 and South Atlantic DSDP Site 525A (Fig. 5). Planktonic foraminiferal $\delta^{18}\text{O}$ values of the late Campanian interval (~ 74 – 72 Ma) at Sites 463 and 525A vary between about $-2\text{\textperthousand}$ and $-1\text{\textperthousand}$ (Fig. 5). Preceding the Campanian–Maastrichtian transition (71.5 Ma) $\delta^{18}\text{O}$ values increased by $\sim 0.3\text{\textperthousand}$ at Site 463, but decreased at Site 525A (Fig. 5). In the early Maastrichtian (70.3 Ma interval) at Site 463 $\delta^{18}\text{O}$ values ranged between $-1.5\text{\textperthousand}$ and $-0.85\text{\textperthousand}$ (Fig. 5) reflecting progressive cooling. The temporary warm event in the early Maastrichtian (69.2–67.3 Ma) observed by Li and Keller (1998a, 1999, figs. 1 and 2) is recorded in the 69.3-Ma sample interval at Site 463 with $\delta^{18}\text{O}$ values between $-1.9\text{\textperthousand}$ and $-1.15\text{\textperthousand}$, reflecting similar climatic conditions as in the late Campanian. The late Maastrichtian global cooling (68.3–65 Ma) is recorded by heavier $\delta^{18}\text{O}$ values at

Plate I.

- 1,2. *Globotruncanita stuartiformis* (Dalbeiz), DSDP Site 577A, sample 13cc, 18–21 cm. Note that there is no test infilling.
3. Detail of the internal surface of *G. stuartiformis* in (1,2) showing secondary recrystallization.
4. *Rugoglobigerina rugosa* (Brönnimann), Site 577A, sample 13-6, 42–44 cm.
- 5,6. Detail of the external surface ridges of *R. rugosa* in (4). Note calcite encrustation on the external surface.
7. *Pseudogrubelina excolata* (Cushman), DSDP Site 463, sample 10-6, 97–100 cm.
8. View of encrusted external surface of *P. excolata* in (7).
9. *Heterohelix punctulata* (Cushman), Site 463, sample 20-1, 100–102 cm. Note absence of test infilling.
10. Cross section of recrystallized wall of *H. punctulata* in (9).
11. *Rosita walfischensis* (Todd), Site 463, sample 10-6, 97–100 cm. Note that there is no or little test infilling.
- 12,13. Cross section of recrystallized surface and wall of *R. walfischensis* in (11).
14. Detail of clean but moderately encrusted external surface of *Abathomphalus mayaroensis* in (15).
15. *Abathomphalus mayaroensis* (Bolli), Site 525A, sample 40-5, 90–92 cm.
16. *Rugoglobigerina rugosa* (Brönnimann), Site 525A, sample 50-1, 100–102 cm.
17. View of moderate encrustation on the external surface of *R. rugosa* in (16).



Site 525A ($-1.2\text{\textperthousand}$ to $-0.5\text{\textperthousand}$) and generally $>0.6\text{\textperthousand}$ enriched at Site 577A relative to the late Campanian at Site 463 (Fig. 5).

Major late Cretaceous global climatic changes are also expressed by the long-term $\delta^{18}\text{O}$ variations recorded by individual planktonic foraminiferal species (Fig. 5). For example, at Site 463, $\delta^{18}\text{O}$ values of *Pseudoguembelina costulata* (Cushman) (Plate II) vary from $-2\text{\textperthousand}$ in the late Campanian (74.3, 72.9 Ma), to $-1.5\text{\textperthousand}$ in the early Maastrichtian (70.3 Ma) and back to $-1.9\text{\textperthousand}$ by 69.3 Ma. Maximum $\delta^{18}\text{O}$ values of *P. costulata* ($-1.35\text{\textperthousand}$ and $-1\text{\textperthousand}$) are recorded in the late Maastrichtian interval (68.3–67.7 Ma) at Site 577A. At the South Atlantic Site 525A, $\delta^{18}\text{O}$ values of *Heterohelix rajagopalani* (Plate II) vary from $-1\text{\textperthousand}$ in the late Campanian (72.3 Ma) to $-0.5\text{\textperthousand}$ in the late Maastrichtian (Fig. 5).

3.2. Late Cretaceous $\delta^{13}\text{C}$ trends

Planktonic foraminiferal $\delta^{13}\text{C}$ values of the equatorial Pacific DSDP Site 463 at the 74.3-Ma and 72.9-Ma sample intervals vary between $2.8\text{\textperthousand}$ and $2.1\text{\textperthousand}$ (Fig. 6). A temporary $\delta^{13}\text{C}$ decrease occurred at 71.5 Ma with values ranging between $\sim 2.5\text{\textperthousand}$ and $1.6\text{\textperthousand}$. Thereafter, $\delta^{13}\text{C}$ values slightly increased, ranging between $2.8\text{\textperthousand}$ and $1.8\text{\textperthousand}$ at the 70.3-Ma and 69.3-Ma intervals (Fig. 6). A significant increase in $\delta^{13}\text{C}$ values to between $3.8\text{\textperthousand}$ and $2.1\text{\textperthousand}$ is observed in the early

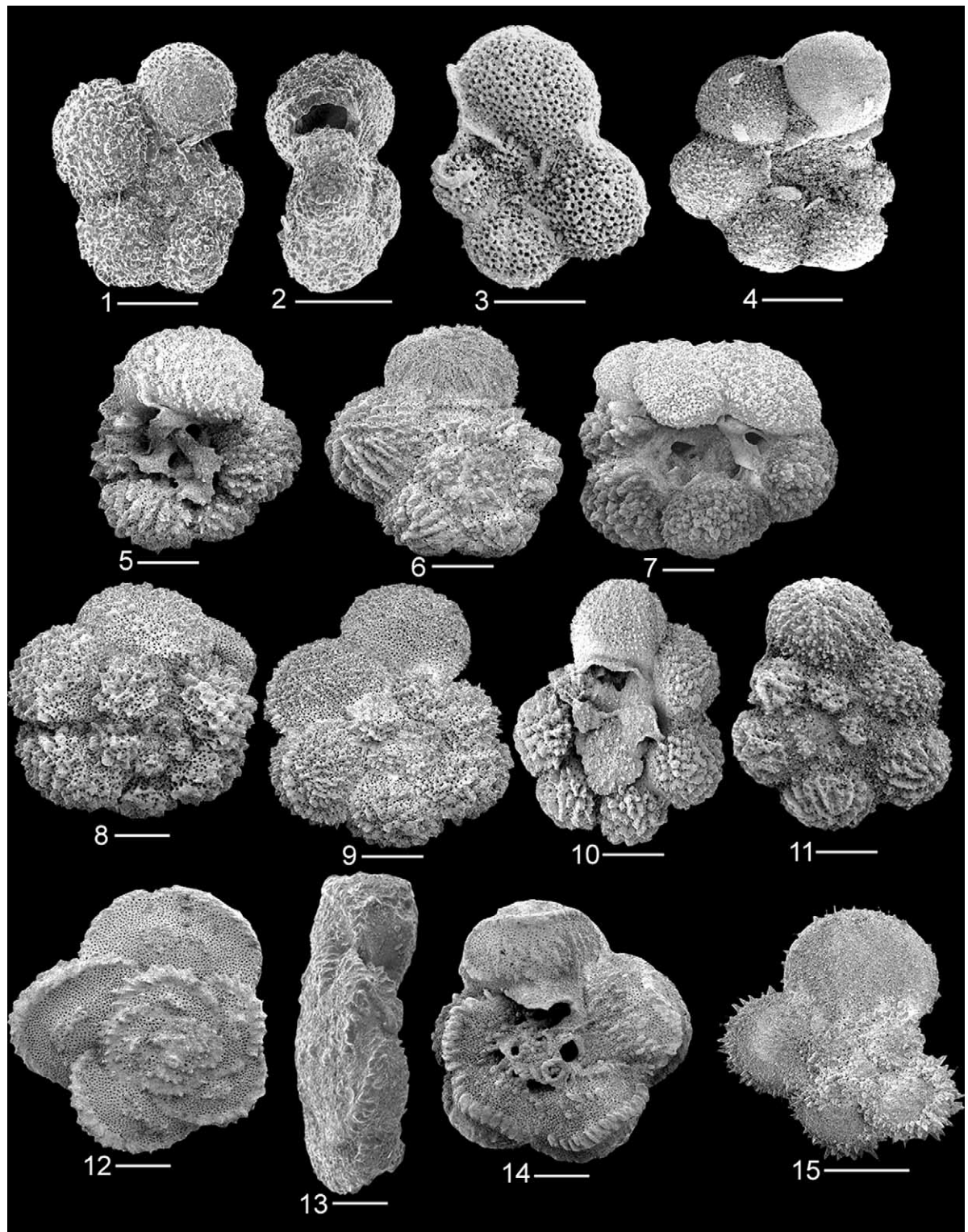
late Maastrichtian interval (between 68.3 Ma and ~ 67 Ma) at both DSDP Sites 577A and 525A (Fig. 6), as also recorded by the $\delta^{13}\text{C}$ values of individual species. For example, at Site 525A $\delta^{13}\text{C}$ values of *Heterohelix rajagopalani* vary from 0.94 – $0.96\text{\textperthousand}$ in the late Campanian (72.3 and 71.5 Ma) to $2.17\text{\textperthousand}$ in the late Maastrichtian 66.8-Ma interval. Similarly, at sites 463 and 577A, $\delta^{13}\text{C}$ values of *Pseudoguembelina costulata* increased by $0.5\text{\textperthousand}$ from the early to the late Maastrichtian (Fig. 6). Similar trends were recorded in middle and southern Atlantic DSDP Sites 525A (Fig. 1), 528, 690, and 689, and in Indian Ocean Site 750 (Barrera and Huber, 1990; Barrera, 1994; Barrera and Keller, 1994; D'Hondt and Lindinger, 1994; Li and Keller, 1998a, 1999; Barrera and Savin, 1999).

During the latest Maastrichtian between 65.6 and 65.1 Ma $\delta^{13}\text{C}$ values decreased at Site 525A with values ranging between $\sim 3.1\text{\textperthousand}$ and $1.8\text{\textperthousand}$ (Fig. 6), as also indicated by the long-term isotopic record (Li and Keller, 1998a,b, fig. 1). This decrease is also observed by the $\delta^{13}\text{C}$ values of *Racemiguembelina powelli* Smith and Pessagno (Plate IV) at Site 525A, which decreased from $3.31\text{\textperthousand}$ at 66.8 Ma to $3.06\text{\textperthousand}$ at 65.6 Ma and to a minimum of $2.92\text{\textperthousand}$ at 65.1 Ma. Similar latest Maastrichtian trends were recorded from other deep-sea localities including equatorial Pacific Site 577 (Zachos et al., 1985, 1989), South Atlantic Sites 690 and 689 (Stott and Kennett,

Plate II.

- 1,2. *Heterohelix globulosa* (Ehrenberg), DSSDP Site 525A, sample 41-6, 89–91 cm.
- 3. *Heterohelix labellosa* (Nederbragt), Site 577A, sample 13-6, 42–44 cm.
- 4. *Heterohelix planata* (Cushman) DSDP Site 463, sample 16-6, 101–103 cm.
- 5. *Heterohelix punctulata* (Cushman), Site 463, sample 20-1, 100–102 cm.
- 6. *Laeviheterohelix glabrans* (Nederbragt), Site 525A, sample 48-3, 100–102 cm.
- 7,8. *Heterohelix rajagopalani* (Govindan), Site 525A, samples 40-5, 50–52 cm, and 40-2, 104–106 cm.
- 9. *Gublerina acuta* (De Klasz), Site 525A, sample 41-6, 89–91 cm.
- 10,11. *Gublerina cuvilli* (Kikoine), Site 577A, sample 13cc, 18–21 cm.
- 12. *Pseudoguembelina costulata* (Cushman), Site 463, sample 13-3, 97–99 cm.
- 13. *Pseudoguembelina excolata* (Cushman), Site 577A, sample 13cc, 18–21 cm.
- 14. *Pseudoguembelina kempensis* (Eskev), Site 577A, sample 13-6, 42–44 cm.
- 15. *Pseudoguembelina hariaensis* (Nederbragt), Site 525A, sample 40-4, 80–82 cm.
- 16–18. *Pseudoguembelina palpebra* (Brönnimann and Brown), Site 525A, 41-6, sample 89–91 cm (16), Site 577A, sample 13-6, 42–44 cm (17–18).

Scale bar = 100 μm



1990), and from several land-based localities in Tunisia (Stüben et al., in press), and Madagascar (Abramovich et al., 2002).

3.3. Intraspecies variation

$\delta^{18}\text{O}$ vs. $\delta^{13}\text{C}$ plots (Fig. 7) reveal maximum intraspecies variation between the warmest late Campanian (74.3–71.5 Ma) and coldest late Maastrichtian (68.3–65.1 Ma) sample intervals (also see Figs. 8 and 9). At the South Atlantic DSDP Site 525A the range of intraspecies $\delta^{18}\text{O}$ and $\delta^{13}\text{C}$ variation between these climatic periods commonly exceeds 0.6‰, and may be as high as 1.3‰, as vividly illustrated in Fig. 8. Intraspecies variations between the late Maastrichtian intervals (68.3–65.1 Ma) of Sites 577A and 525A mostly range between 0.2‰ and 0.4‰. $\delta^{18}\text{O}$ and $\delta^{13}\text{C}$ values of most species in the late Maastrichtian intervals are typically more enriched at Site 577A than at Site 525A (Figs. 7–9). In addition, most late Maastrichtian planktonic foraminiferal species show low intraspecies variations (0.1–0.2‰) within samples of the same site (Fig. 7). Notable exceptions are the wide isotopic variations recorded by *Racemiguembelina* spp., *Pseudoguembelina* spp. (Site 577A), *Heterohelix globulosa* (Site 525A) and *Rugoglobigerina pennyi* Brönnimann (Site 525A; Fig. 8).

Late Campanian intervals of Sites 525A and 463 show greater intraspecies variation between localities and within samples of the same site than late Maastrichtian intervals (Fig. 7). For example, in the 71.5-Ma interval, the range of intra-

species $\delta^{18}\text{O}$ and $\delta^{13}\text{C}$ variation between Sites 525A and 463 is commonly >0.5‰ and >0.3‰, respectively, and occasionally exceeds 1‰ ($\delta^{18}\text{O}$ keeled globotruncanids; Figs. 7 and 8). Similarly, *Globotruncana linneiana* (d'Orbigny) shows 0.96‰ variation in $\delta^{18}\text{O}$ between 74.3 and 72.9 Ma at Site 463. These ranges reflect an overall isotopic species enrichment at Site 463 relative to Site 525A, as well as variations in the relative isotopic ordering of some species (see Section 3.4).

3.4. Relative $\delta^{18}\text{O}$ ranking

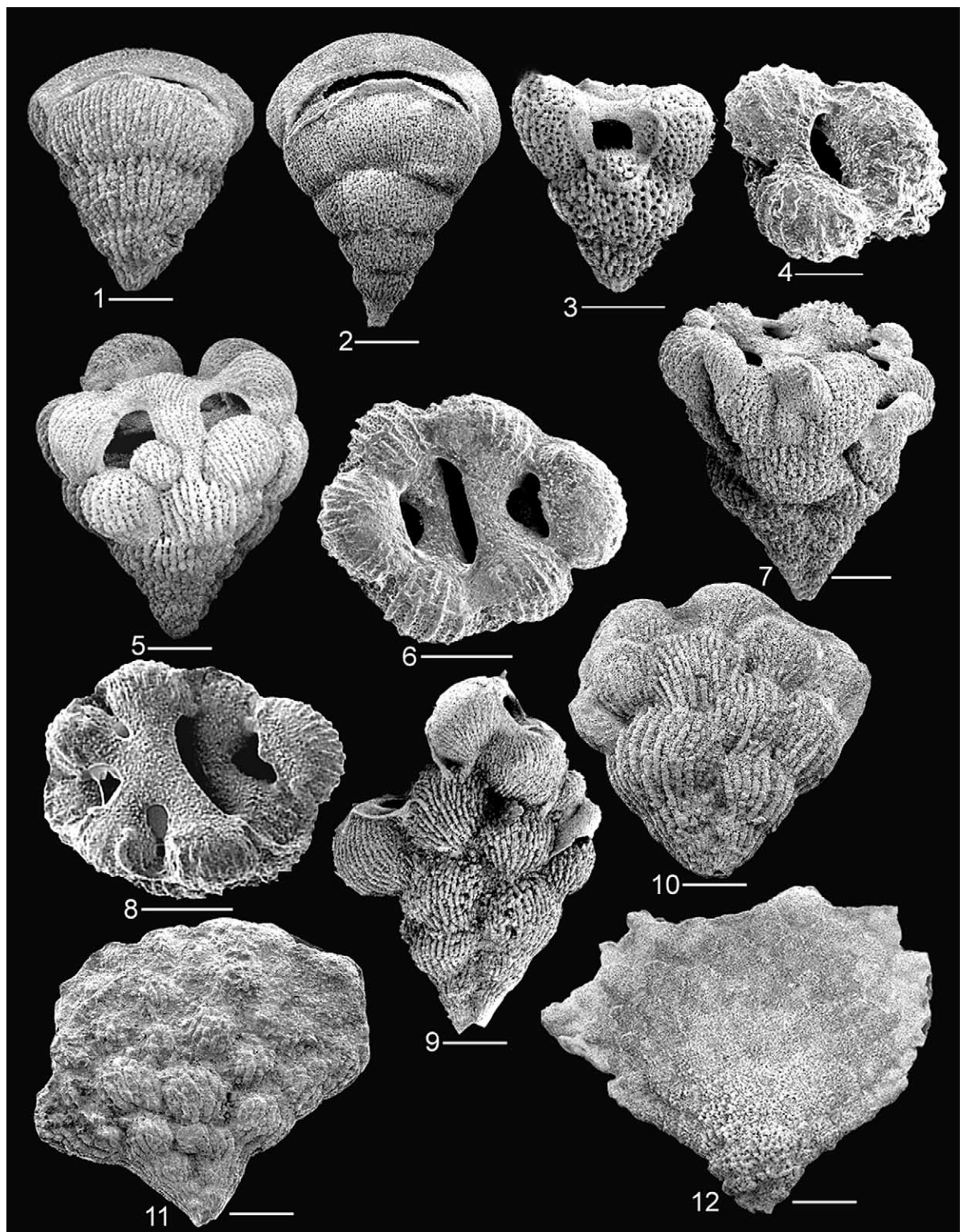
$\delta^{18}\text{O}$ ranking of species in the late Maastrichtian sample intervals of equatorial Pacific Site 577A and South Atlantic Site 525A demonstrates that all members of the genus *Pseudoguembelina* (e.g. *P. costulata*, *P. excolata*, *P. hariaensis* Nederbragt, *P. kempensis* Esker and *P. palpebra* Brönnimann and Brown; Plate II) are consistently lighter than most coexisting species (Figs. 7 and 8). The same isotopic ranking of this genus is recorded in the late Campanian and early Maastrichtian intervals of Site 463, where $\delta^{18}\text{O}$ values of *P. costulata* are lighter than most coexisting species.

At Site 525A the endemic species *Heterohelix rajagopalani* (Plate II) defines the opposite extreme of the $\delta^{18}\text{O}$ ranking during the late Maastrichtian and late Campanian, with $\delta^{18}\text{O}$ values typically heavier than all other taxa, except for *Globotruncanita stuartiformis* (Dalbiez) in the 65.1-Ma interval (Figs. 7 and 8). At Site 577A *Planoglobulina multicamerata* (Plate IV) shows

Plate III.

- 1,2. *Globigerinelliodes aspera* (Ehrenberg), DSDP Site 525A, sample 40-5, 90–92 cm.
3. *Globigerinelliodes subcarinatus* (Brönnimann), Site 577A, sample 13-6, 42–44 cm.
4. *Globigerinelloides* aff. *ultramicros* (Subbotina), DSDP Site 463, sample 16-6, 101–103 cm.
- 5,6. *Rugoglobigerina rugosa* (Brönnimann), Site 577A, sample 13-6, 42–44 cm.
- 7,8. *Rugoglobigerina rotundata* (Brönnimann), Site 577A, sample 13cc, 18–21 cm.
- 9,10. *Rugoglobigerina scotti* (Brönnimann), Site 577A, sample 13-6, 42–44 cm.
11. *Rugoglobigerina hexamerata* (Brönnimann), Site 525A, 41-6, sample 89–91 cm.
- 12–14. *Abathomphalus mayaroensis* (Bolli), Site 525A, samples 40-5, 90–92 cm (11), and 41-6, sample 89–91 cm (12,13).
15. *Globotruncanella havanensis* (Voorwijk), Site 525A, sample 40-2, 104–106 cm.

Scale bar = 100 µm



the heaviest $\delta^{18}\text{O}$ values. This species evolved only in the later part of the Maastrichtian and was generally restricted to low latitudes (e.g. not present at Sites 463 and 525A; Nederbragt, 1998). The two morphovariants of the *Globotruncanella*–*Abathomphalus* lineage, *G. havanensis* and *A. mayaroensis* (see Robaszynski et al., 1983–1984, and Plate III), and the species *Laeviheterohelix glabrans* and *Gublerina cuvillieri* (Plate II) also show relatively heavy $\delta^{18}\text{O}$ values, though lighter than *P. multicamerata* at Site 577A and *H. rajagopalani* at Site 525A (Figs. 7 and 8).

Species with intermediate $\delta^{18}\text{O}$ values show distinct ordering in late Maastrichtian intervals at Sites 577A and 525A. Within this group, $\delta^{18}\text{O}$ values of *Pseudotextularia* spp., *Planoglobulina* spp. (except *P. multicamerata*; Plate IV), and *Rugoglobigerina* spp. (Plate III) generally overlap and are relatively heavier than *Pseudoguembelina* species and lighter than most keeled globotruncanids (Fig. 8 and details in Fig. 7). *Rosita walfischensis* (Todd) and *Globotruncana rosetta* (Carsey) at Site 577A next to *Globotruncana mariei* Banner and Blow (Plate V) at Site 525A show $\delta^{18}\text{O}$ values similar to or lighter than *Rugoglobigerina*. Among keeled globotruncanids (Plate V), $\delta^{18}\text{O}$ values of *Globotruncanita stuartiformis* are consistently heavier than those of *Globotruncana arca* (Cushman) in the late Maastrichtian intervals of both Sites 577A and 525A.

$\delta^{18}\text{O}$ ordering of keeled globotruncanids in the late Campanian and early Maastrichtian intervals is less distinct than observed in late Maastrichtian intervals. At Site 463, $\delta^{18}\text{O}$ values of most keeled

globotruncanids (except *Globotruncana linneiana*) are heavier or overlap with those of *Rugoglobigerina* (Fig. 8). Most extreme variations in the $\delta^{18}\text{O}$ of keeled globotruncanids are observed in the late Campanian of Site 525A, where most species of this group (except *G. arca*) show exceptionally depleted $\delta^{18}\text{O}$ values (Figs. 7 and 8).

Strong variation in relative $\delta^{18}\text{O}$ ranking is also recorded by *Racemiguembelina* spp. (Plate IV), *Globigerinelloides* spp. (Plate III), and the dominant Maastrichtian species *Heterohelix globulosa* (Plate II). For example, late Maastrichtian $\delta^{18}\text{O}$ values of *Globigerinelloides aspera* (Ehrenberg) and *H. globulosa* are typically lighter than those of most keeled globotruncanids at Site 577A, and in the 65.1-Ma interval at Site 525A (Figs. 7 and 8). On the other hand, in the 66.8-Ma and 65.6-Ma intervals at Site 525A, $\delta^{18}\text{O}$ values of these species are considerably more enriched. The $\delta^{18}\text{O}$ ordering of *Racemiguembelina* spp. varies from similar ranking as *Pseudoguembelina* spp. at the 66.8-Ma interval at Site 525A to intermediate ranking of keeled globotruncanids at Site 577A.

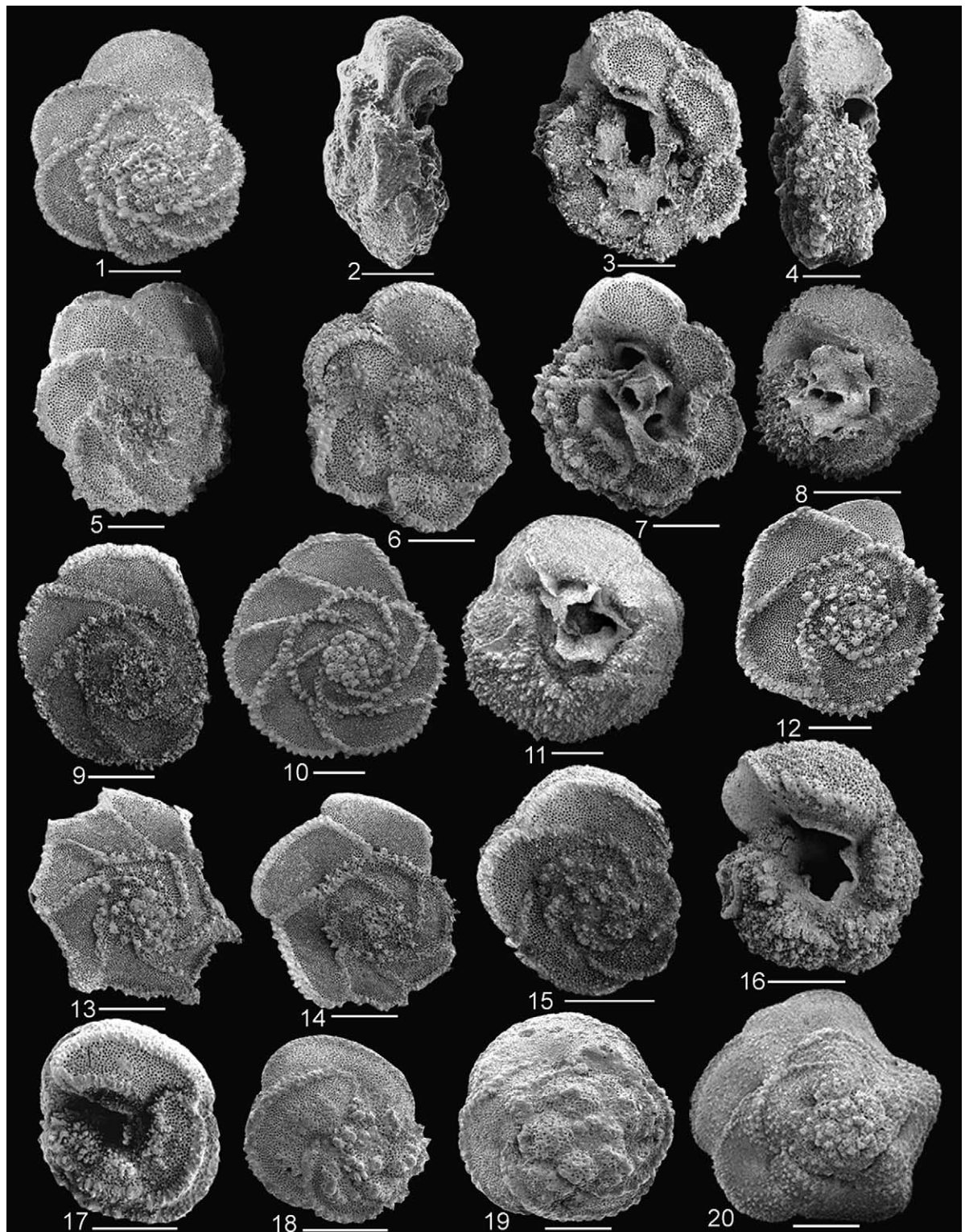
3.5. Relative $\delta^{13}\text{C}$ ranking

The $\delta^{13}\text{C}$ values of the late Maastrichtian *Racemiguembelina* lineage (i.e. *Racemiguembelina fructicosa* (Egger), *R. powelli*, *R. intermedia* De Klasz; Plate IV) are consistently more enriched than most other species in the Atlantic and Pacific, and are typically more depleted in the South Atlantic DSDP Site 525A than in the equatorial Pacific DSDP Site 577A (particularly 65.1 Ma;

Plate IV.

1. *Pseudotextularia deformis* (Kikoine), DSDP Site 577A, sample 13cc, 18–21 cm.
2. *Pseudotextularia elegans* (Rzehak), Site 525A, 41-6, sample 89–91 cm.
- 3.4. *Racemiguembelina intermedia* (De Klasz), Site 577A, sample 13-6, 42–44 cm.
- 5.6. *Racemiguembelina powelli* (Smith and Pessagno), sample 40-5, 90–92 cm.
- 7.8. *Racemiguembelina fructicosa* (Egger), Site 577A, sample 13cc, 18–21 cm (7), and Site 525A, sample 41-6, 89–91 cm (8).
9. *Planoglobulina carseyae* (Plummer), Site 577A, sample 13cc, 18–21 cm.
10. *Planoglobulina brazoensis* (Martin), Site 525A, sample 40-2, 104–106 cm.
11. *Planoglobulina acervulinoides* (Egger), Site 577A, sample 13-6, 42–44 cm.
12. *Planoglobulina multicamerata* (De Klasz), Site 577A, sample 13cc, 18–21 cm.

Scale bar = 100 μm



Figs. 7 and 9). Within the *Racemiguembelina* lineage, the largest youngest and most developed morphovariant *R. fructicosa* shows the heaviest $\delta^{13}\text{C}$ values, whereas the $\delta^{13}\text{C}$ values of *R. powelli* are typically lighter than those of *R. fructicosa* and mostly heavier than those of *R. intermedia* (Figs. 7 and 9). The latter defines a transitional form between *R. powelli* and the species *Pseudotextularia deformis* (Kikoine), a probable ancestor of the *Racemiguembelina* lineage (Smith and Pessagno, 1983). At Site 577A, the $\delta^{13}\text{C}$ values of *P. deformis* are relatively enriched compared with most species, and lighter than those of *R. intermedia*. In contrast, in the late Maastrichtian at Site 525A, *P. deformis* shows intermediate $\delta^{13}\text{C}$ values at the 65.1-Ma and 65.6-Ma intervals.

Other species that typically display relatively enriched $\delta^{13}\text{C}$ values include all morphotypes of the *Rosita* (i.e. *Rosita patelliformis* (Gandolfi), *Rosita Plicata* (White), *Rosita plummerae* (Gandolfi), *R. walfischensis*; Plate V) and *Planoglobulina* groups (except *P. multicamerata*; Figs. 7 and 9). In the late Maastrichtian intervals at Site 577A, the $\delta^{13}\text{C}$ values of *Planoglobulina* species generally overlap with those of *Racemiguembelina intermedia*, but at Site 525A they are significantly more depleted. *Rosita* species overlap with *Planoglobulina* at Site 577A and *Racemiguembelina powelli* at Site 525A. *Rugoglobigerina* species display enriched $\delta^{13}\text{C}$ values in the late Campanian and

early Maastrichtian intervals at Site 463, but intermediate values in the late Campanian intervals at Site 525A and at Site 577A (Figs. 7 and 9). Other species with intermediate $\delta^{13}\text{C}$ ranking include all members of the keeled globotruncanid group, *Pseudotextularia elegans*, *Heterohelix globulosa* and species of the genera *Globigerinelloides* and *Pseudoguembelina*. Among *Pseudoguembelina* species, the $\delta^{13}\text{C}$ values of *P. kempensis* and *P. costulata* are typically more depleted than those of *P. excolata* and *P. palpebra* (Figs. 7 and 9).

Species that consistently display relatively depleted $\delta^{13}\text{C}$ values include *Abathomphalus mayaroensis* (at Site 525A), *Planoglobulina multicamerata* (Site 577A), *Globotruncanella havanensis*, *Gublerina acuta* and *Heterohelix planata*. Within this group, the late Maastrichtian species *A. mayaroensis* (Plate III) exhibits the most depleted values at both Pacific and Atlantic sites (Figs. 7 and 9). The species *P. multicamerata* (Plate IV), *Heterohelix rajagopalani* (Plate II) are typically heavier than *A. mayaroensis* but lighter than *G. havanensis* (except in 65.1 Ma; Fig. 7).

4. Discussion

4.1. Diagenesis and paleotemperature

The presence of secondary recrystallization and

Plate V.

- 1,2. *Globotruncana arca* (Cushman), DSDP Site 525A, sample 48-3, 100–102 cm.
- 3–5. *Globotruncana linneiana* (d'Orbigny), DSDP Site 463, sample 20-1, 100–102 cm.
6. *Globotruncana bulloides* (Vogler), Site 463, sample 16-6, 101–103 cm.
7. *Globotruncana orientalis* (El Naggar), Site 577A, sample 13cc, 18–21 cm.
8. *Globotruncana aegyptiaca*, Site 577A, sample 13-6, 42–44 cm.
9. *Globotruncanita angulata* (Tilev), Site 577A, sample 13cc, 18–21 cm.
- 10,11. *Globotruncanita stuarti* (De Lapparent), Site 463, sample 13-3, 97–99 cm.
12. *Globotruncanita stuartiformis* (Dalbiez), Site 577A, sample 13-6, 42–44 cm.
13. *Globotruncanita calcarata* (Cushman), Site 463, sample 21-5, 64–66 cm.
14. *Globotruncanita subspinosa* (Pessagno), Site 463, sample 21-5, 64–66 cm.
- 15,16. *Gansserina gansseri* (Bolli), Site 463, sample 13-3, 97–99 cm.
17. *Rosita fornicata* (Plummer), Site 463, sample 21-5, 64–66 cm.
18. *Rosita plummerae* (Gandolfi), Site 525A, sample 50-1, 100–102 cm.
19. *Rosita walfischensis* (Todd), Site 463, sample 10-6, 97–100 cm.
20. *Rosita patelliformis* (Gandolfi), Site 577A, sample 13-6, 42–44 cm.

Scale bar = 100 μm

Table 3

Classification of late Cretaceous planktonic foraminiferal species into mixed layer (surface, subsurface), thermocline, and sub-thermocline (deep) dwellers: (A) coldest late Maastrichtian; (B) cool early Maastrichtian in the equatorial Pacific; (C) warmest late Campanian interval

	mixed layer		thermocline	sub-thermocline (deep)
	surface	subsurface		
A. Late Maastrichtian coldest intervals	<i>Pseudoguembelina excolata</i> <i>P. kempensis</i> <i>P. costulata</i> <i>P. hariaensis</i> <i>P. palpebra</i> <i>Rugoglobigerina hexacamerata</i> (65.6) <i>R. pennyi</i> (65.1) <i>Planoglobulina acervulinoides</i>	<i>Globotruncana aegyptiaca</i> <i>G. mariei</i> (65.1) <i>G. rosetta</i> <i>Rosita walfischensis</i> <i>Rugoglobigerina rugosa</i> <i>R. hexacamerata</i> <i>R. milamensis</i> <i>R. rotundata</i> <i>Globigerinelloides aspera</i> <i>G. subcarinatus</i> <i>Gublerina acuta</i> <i>Pseudotextularia deformis</i> <i>P. elegans</i> <i>Heterohelix globulosa</i> <i>H. labellosa</i> <i>Planoglobulina carseyae</i> <i>P. acervulinoides</i> <i>P. brazoensis</i>	<i>Globotruncana arca</i> <i>G. duepeblei</i> <i>G. falsostuarti</i> <i>G. mariei</i> <i>G. orientalis</i> <i>G. ventricosa</i> <i>Globotruncanita angulata</i> <i>G. stuarti</i> <i>Rosita patelliformis</i> <i>Racemiguembelina fructicosa</i> <i>R. intermedia</i> <i>R. powelli</i> <i>Rugoglobigerina pennyi</i> (66.8) <i>Heterohelix globulosa</i> (66.8, 65.6) <i>Globigerinelloides aspera</i>	<i>Planoglobulina multicamerata</i> <i>Heterohelix rajagopalani</i> <i>Abathomphalus mayaroensis</i> <i>Globotruncanella havanensis</i> <i>Gublerina cuvillieri</i> <i>Globotruncana stuartiformis?</i>
B. Early Maastrichtian cool interval (70.3 Ma)	<i>Pseudoguembelina costulata</i> <i>Gublerina acuta</i>	<i>Globotruncana bulloides</i> <i>G. linneiana</i> <i>Rugoglobigerina rugosa</i> <i>R. hexacamerata</i> <i>Globigerinelloides aspera</i> <i>G. aff. ultramicro</i> <i>Pseudotextularia elegans</i> <i>Heterohelix globulosa</i> <i>H. punctulata</i> <i>H. planata</i>	<i>Globotruncana aegyptiaca</i> <i>G. arca</i> <i>G. insignis</i> <i>G. stuarti</i> <i>G. ventricosa</i> <i>Globotruncanita angulata</i> <i>Gansserina gansseri</i>	?
C. Late Campanian warmest intervals	<i>Pseudoguembelina costulata</i> <i>Globotruncana aegyptiaca</i> <i>G. bulloides</i> <i>G. linneiana</i> <i>Rosita plummerae</i>	<i>Globotruncanita calcarata</i> <i>G. stuarti</i> <i>G. stuartiformis</i> <i>G. subspinosa</i> <i>Globotruncana arca</i> <i>G. bulloides</i> <i>G. linneiana</i> <i>Rosita plummerae</i> <i>Pseudotextularia elegans</i> <i>Heterohelix globulosa</i> <i>H. planata</i> <i>Globigerinelloides aspera</i> <i>G. aff. ultramicro</i> <i>Gublerina acuta</i>		<i>Heterohelix rajagopalani</i> <i>Laeviheterohelix glabrans</i>

Gray shaded species display different depth ranking in the mid-latitude Atlantic than in the equatorial Pacific. Intermediate dwelling species in the late Campanian are not further classified due to the high isotopic variations in the mid-latitude Atlantic, and isotopic overlap in the equatorial Pacific (see Fig. 7).

calcite overgrowth of foraminiferal tests implies early diagenesis under low temperature conditions and a positive $\delta^{18}\text{O}$ shift towards heavier (cooler) values (Wu and Berger, 1990; Schrag et al., 1995; Schrag, 1999; Pearson et al., 2001). Pearson et al. (2001) argued that up to 50% of the original calcite can be replaced by early diagenetic calcite even in well preserved foraminiferal tests and the subsequent positive shift in planktonic foraminiferal $\delta^{18}\text{O}$ values can reduce paleotemperature

estimates by up to 10–15°C. Early diagenetic effects are expected to be most pronounced in deep water carbonates of low latitudes, because surface dwelling planktonic foraminifera of tropical oceans are prone to diagenetic overprints due to the large $\delta^{18}\text{O}$ differences between their original $\delta^{18}\text{O}$ values and the values in equilibrium with the cold bottom water (Schrag et al., 1995; Schrag, 1999; Pearson et al., 2001).

Early diagenesis can explain the relatively low

sea-surface temperatures (SST) estimated for the late Cretaceous equatorial Pacific DSDP Sites 463 and 577A by D'Hondt and Arthur (1996), Barrera and Savin (1999), Li and Keller (1999), and this study. For example, at Site 577A the maximum late Maastrichtian SST ($\sim 19^{\circ}\text{C}$; Fig. 5) is about 8°C cooler than the modern average SST at this locality (Schweitzer, 1993). Similarly, at Site 463 the maximum late Campanian SST is about 6.5°C cooler than the modern average SST at this locality ($\sim 28^{\circ}\text{C}$; Fig. 5). On the other hand, the maximum SSTs at the South Atlantic DSDP Site 525A are generally 2°C warmer than the average modern SST at this locality ($\sim 16^{\circ}\text{C}$), and 7°C warmer in the late Campanian interval (Fig. 5). These relatively small temperature differences, in addition to the error introduced by secondary re-

crystallization and calcite overgrowths at Site 525A (Plate I), suggest that the original late Cretaceous SSTs at this locality were probably significantly warmer than the calculated values.

Temperature differences recorded between the Pacific Sites 577A and 463 and the Atlantic Site 525A demonstrate that the SST gradients between the equatorial and middle latitudes were particularly low and even inverse to the modern SST gradient. For example, at 71.5 Ma the maximum SST at Site 525A was about 3°C warmer than at Site 463, and only $\sim 1.5^{\circ}\text{C}$ cooler than at Site 577A in the late Maastrichtian (Fig. 5). This trend is considerably different from the average modern geographic gradient that records as much as $\sim 11^{\circ}\text{C}$ decrease in SSTs between the equator and 36°S (Schweitzer, 1993). D'Hondt and Arthur

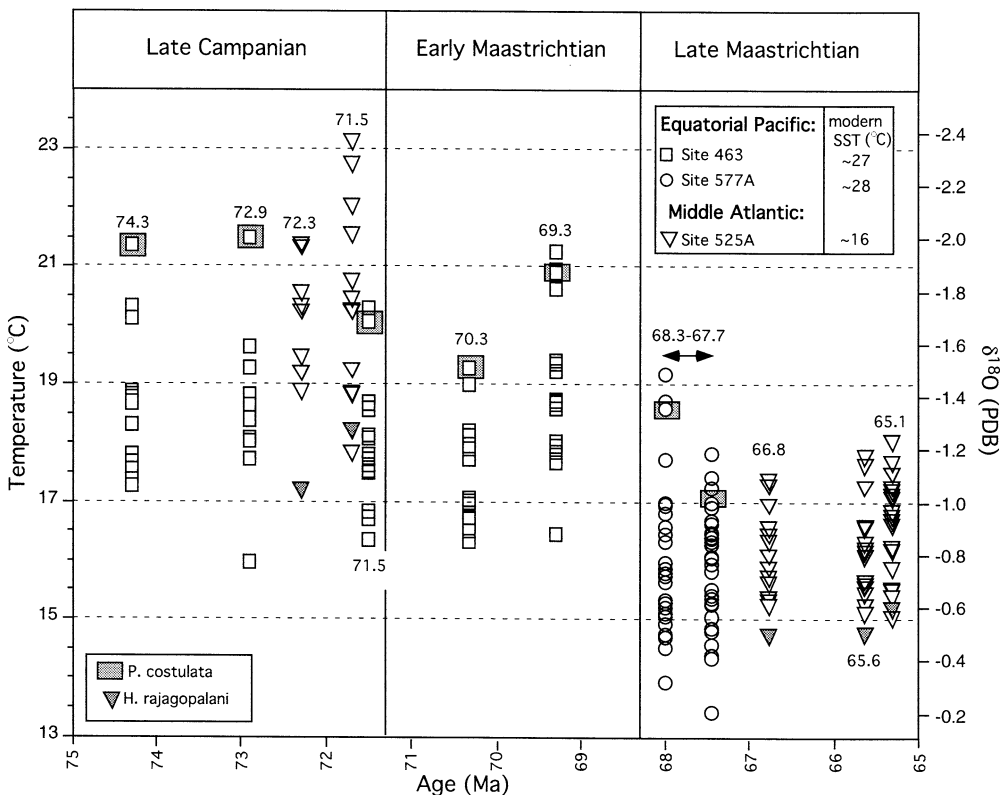


Fig. 5. Oxygen isotope and paleotemperature records of the eleven sample intervals selected from DSDP Sites 463 and 577A (equatorial Pacific) and DSDP Site 525A (South Atlantic). Note that the substantially cooler temperatures of the latest Maastrichtian intervals are also demonstrated by the $\delta^{18}\text{O}$ trends of *Pseudoguembelina costulata* and *Heterohelix rajagopalani*. Also note that maximum late Cretaceous temperatures are mostly cooler than the modern average SST (particularly in the equatorial Pacific), indicating the effect of bottom deep-sea diagenesis. Modern SST data from Schweitzer (1993).

(1996) suggested that the reduced latitudinal SST gradient in the late Cretaceous resulted from a greater heat transport from the tropics to higher latitudes. However, such a mechanism cannot explain the inverse SST gradient recorded between Sites 525A and 463 at 71.5 Ma, which suggests that diagenetic alteration in the tropics is partly responsible for the observed late Cretaceous SST gradient.

4.2. Depth ranking

4.2.1. Deep dwellers

$\delta^{18}\text{O}$ values of foraminiferal calcite generally increase with depth due to decreasing temperatures (Fairbanks et al., 1982), and $\delta^{13}\text{C}$ values decrease with depth due to selective removal of

^{12}C by photosynthesis in the photic zone and accumulation of ^{12}C in deeper water due to organic matter decay (Bouvier-Soumagnac and Duplessy, 1985). Accordingly, deep planktonic foraminiferal species are expected to display the heaviest $\delta^{18}\text{O}$ and lightest $\delta^{13}\text{C}$ values, characteristic of cold and respiration-dominated environments below the thermocline.

Deep dwellers identified in this study include *Planoglobulina multicamerata*, *Heterohelix rajagopalani*, *Abathomphalus mayaroensis*, *Globotruncanella havanensis* and *Gublerina cuvillieri* in the late Maastrichtian, and *Heterohelix rajagopalani* and *Laeviheterohelix glabrans* in the Late Campanian (Plates II–IV; Table 3). No deep dwellers were analyzed for the early Maastrichtian. The tropical species *Planoglobulina multicamerata* (Figs. 7 and

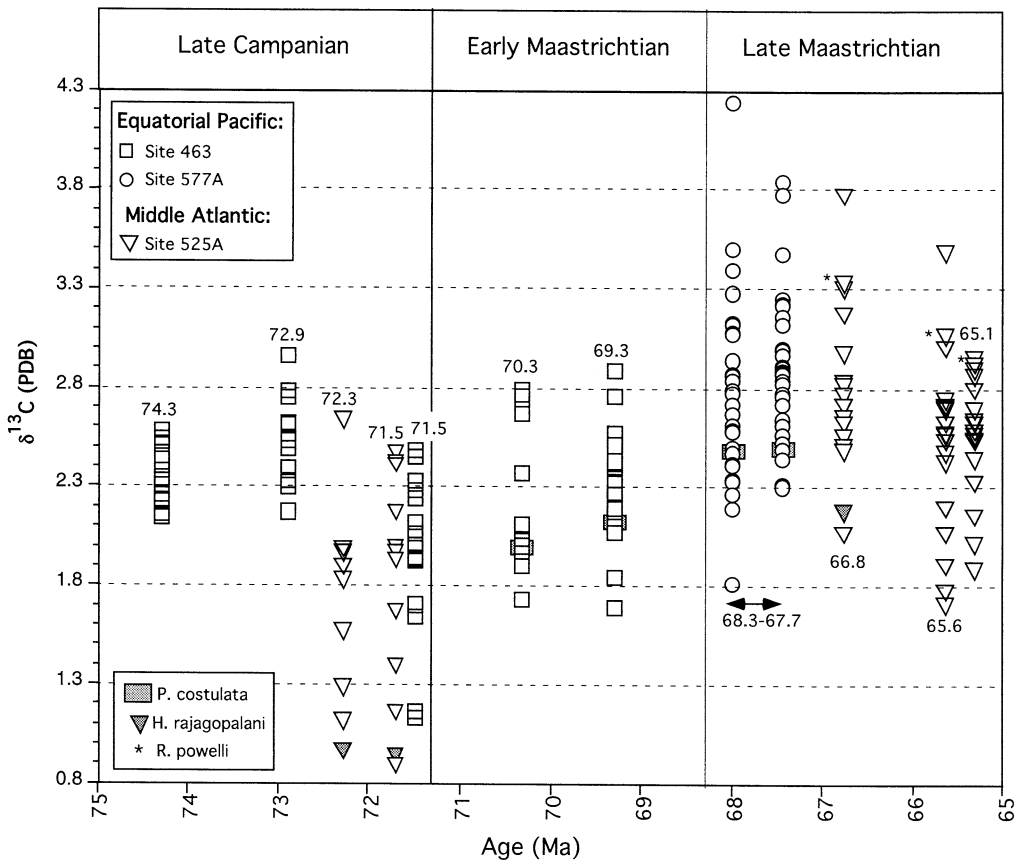


Fig. 6. Carbon isotope records of the eleven sample intervals selected from DSDP Sites 463 and 577A (equatorial Pacific) and 525A (South Atlantic). Note the $\delta^{13}\text{C}$ increase in the early–late Maastrichtian indicated by the species *Pseudoguembelia costulata* and *Heterohelix rajagopalani*, and the decrease in the latest Maastrichtian indicated by *Racemiguembelia powelli* at Site 525A.

8) has the heaviest $\delta^{18}\text{O}$ values and apparently inhabited the deepest and coldest plankton habitat in the equatorial Pacific (Table 3) and other localities (e.g. Douglas and Savin, 1978; Boersma and Shackleton, 1981; D'Hondt and Arthur, 1995; D'Hondt and Zachos, 1998; Houston and Huber, 1998; Houston et al., 1999). The endemic species *H. rajagopalani* (Plate II) inhabited the deepest and coldest plankton habitat in the South Atlantic throughout the late Cretaceous (Table 3), as indicated by $\delta^{18}\text{O}$ and relatively depleted $\delta^{13}\text{C}$ signals (Figs. 7 and 9; see also D'Hondt and Arthur, 1995).

The cosmopolitan late Maastrichtian species *Abathomphalus mayaroensis* (Plate III) inhabited somewhat shallower depths than *Heterohelix rajagopalani* in the South Atlantic, and *Planogobulina multicamerata* in the equatorial Pacific, as indicated by lighter $\delta^{18}\text{O}$ signals (Table 3; Figs. 7 and 8). Similar results are reported from the North and South Atlantic Sites 390A and 20C (D'Hondt and Arthur, 1995), though Pearson et al. (2001) reported intermediate $\delta^{18}\text{O}$ ranking for *A. mayaroensis* in one sample from Lindi, Tanzania. The reason for the discrepancy between the deep-sea $\delta^{18}\text{O}$ localities and the Tanzania sample is unclear and needs further evaluation. $\delta^{13}\text{C}$ values of *A. mayaroensis* in all localities are significantly lighter than most other species (Figs. 7 and 9). The relatively shallower depth habitat of *A. mayaroensis* with respect to *H. rajagopalani* and *P. multicamerata* suggests that the low $\delta^{13}\text{C}$ values record conditions other than a deep ambient environment (see discussion in Section 4.3.2).

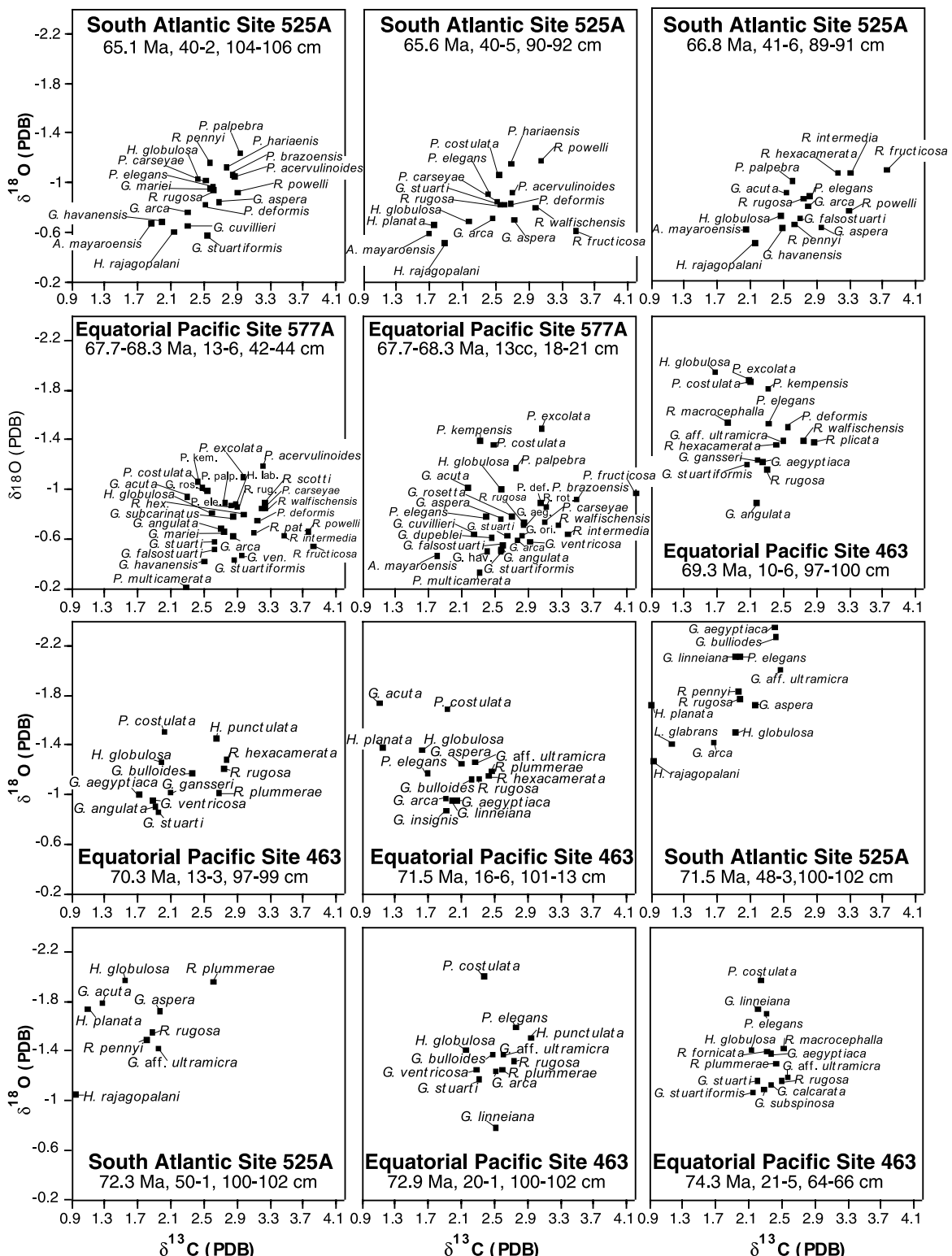
The $\delta^{18}\text{O}$ values of *Globotruncanella havanensis* (Plate III), the ancestor of the *Globotruncanella–Abathomphalus* lineage, indicate a similar water depth as *Abathomphalus mayaroensis* (Figs. 7 and 8; Table 3), as also reported by D'Hondt and Arthur (1995). The $\delta^{18}\text{O}$ values *Gublerina cuvillieri* (Plate II) suggest shallower depths than for *A. mayaroensis* in the equatorial Pacific, but similar depths in the South Atlantic (Figs. 7 and 8). *Laeviheterohelix glabrans* (Plate II) also indicates a deeper water habitat than most other species in the South Atlantic Site 525A (Figs. 7 and 8; see also D'Hondt and Arthur, 1995).

4.2.2. Thermocline dwellers

Species living in the thermocline layer are defined by their intermediate $\delta^{18}\text{O}$ signals, with $\delta^{13}\text{C}$ values generally heavier than for deep dwellers, reflecting primary productivity at these depths. This group includes most keeled globotruncanids (Plate V), *Globigerinelloides* spp. (at Site 525A; Plate III), and *Heterohelix globulosa* (late Maastrichtian, Site 525A; Table 3). The $\delta^{18}\text{O}$ trends recorded among these species suggest that during the late Maastrichtian intervals analyzed most keeled globotruncanids inhabited the deeper or cooler thermocline layer. The $\delta^{18}\text{O}$ variation among keeled globotruncanids suggests that during the late Maastrichtian *Globotruncana arca* inhabited somewhat shallower depths than *Globotruncanita stuartiformis* (Figs. 7 and 8; Table 3), as earlier observed by Douglas and Savin (1978). During the warm late Campanian and early Maastrichtian in the equatorial Pacific most keeled globotruncanids inhabited intermediate to subsurface depths (Table 3). In contrast, during the warm late Campanian interval of South Atlantic Site 525A most keeled globotruncanids (except *G. arca*) inhabited the shallowest water depth as suggested by their exceptionally depleted $\delta^{18}\text{O}$ values (Figs. 7 and 8). This pattern could be explained by absence of a distinct thermocline layer during the warm late Campanian interval in the South Atlantic.

The $\delta^{18}\text{O}$ values of the *Racemiguembelina* species are highly variable, implying a wide range between thermocline to surface depth habitats. However, a possible source for the wide $\delta^{18}\text{O}$ range of *Racemiguembelina* is the vital effect of photosymbiotic activity, which typically results in a negative $\delta^{18}\text{O}$ shift from the ambient water environment (e.g. Spero and Deniro, 1987; Spero, 1992, discussed below).

Late Maastrichtian $\delta^{18}\text{O}$ records of *Globigerinelloides* species suggest that they inhabited somewhat shallower depths than most keeled globotruncanids in the equatorial Pacific (Fig. 7; Table 3). However, in the South Atlantic Site 525A, the $\delta^{18}\text{O}$ values of this species are generally more enriched and correspond to temperatures as cold as those of the deep dwellers *Abathomphalus mayaroensis*, and *Globotruncanella havanensis*.



(Figs. 7 and 8). Similarly, *Heterohelix globulosa* changed habitats between localities and during different climate modes. For example, in the late Maastrichtian 66.8-Ma and 65.6-Ma intervals of South Atlantic Site 525A, the $\delta^{18}\text{O}$ values of *H. globulosa* are as enriched as those of the deep dweller *A. mayaroensis* (Figs. 7 and 8; Table 3), suggesting a relatively cool or deep environment (Table 3). On the other hand, in the 65.1-Ma interval at Site 525A and the equatorial Pacific the $\delta^{18}\text{O}$ values of *H. globulosa* are more depleted and correspond to subsurface depths.

4.2.3. Mixed layer dwellers

Mixed layer dwellers are primarily defined by their depleted $\delta^{18}\text{O}$ signals, which reflect the warm temperatures of the oceans' mixed layer. These $\delta^{13}\text{C}$ signals are typically heavier than those for deep dwellers. In every late Cretaceous planktonic foraminiferal assemblage analyzed *Pseudoguembelina* species (*P. excolata*, *P. costulata*, *P. kempensis*, *P. hariaensis*, *P. palpebra*) and *Gublerina acuta* (Plate II) display the most $\delta^{18}\text{O}$ depleted values, suggesting that they inhabited the warmest or shallowest parts of the mixed layer (Figs. 7 and 8; Table 3). In addition, *Pseudoguembelina* species are also considerably more common in the equatorial Pacific Sites 577A and 463 than in the South Atlantic Site 525A (except for *P. palpebra* and *P. hariaensis*), which suggests that they were optimally adapted to warm temperatures at low latitudes (see also Malmgren, 1991; Nederbragt, 1998). Similarly depleted $\delta^{18}\text{O}$ values were also observed by Douglas and Savin (1978) and Boersma and Shackleton (1981) from Atlantic and Pacific deep sea sites, although D'Hondt and Arthur (1995) reported intermediate depths for *Pseudoguembelina* species at South Atlantic Site 20C. The relatively enriched $\delta^{13}\text{C}$ values of *P. excolata* (and perhaps *P. palpebra*) may reflect some

degree of photosymbiotic activity (see discussion below).

The $\delta^{18}\text{O}$ trends recorded by species of the genera *Rugoglobigerina*, *Pseudotextularia*, and *Planoglobulina* (except *P. multicamerata*) suggest that they generally inhabited somewhat deeper depths than *Pseudoguembelina* species but shallower depths than most keeled globotruncanids during the late Maastrichtian in the South Atlantic and equatorial Pacific (Figs. 7 and 8). During this period, the subsurface environment in the equatorial Pacific was also populated by *Heterohelix globulosa* and *Globigerinelloides* spp. (see discussion above), in addition to several keeled globotruncanids (e.g. *Globotruncana rosetta*). Furthermore, the relatively depleted $\delta^{18}\text{O}$ signals of planktonic foraminifera in the late Campanian intervals, and the lack of a distinct isotopic ordering among *Rugoglobigerina* spp., *Globigerinelloides* spp., *Pseudotextularia* and keeled globotruncanids imply weak upper water-mass stratification and absence of a permanent thermocline layer. Most planktonic foraminifera probably inhabited surface and subsurface depths during this relatively warm climatic period.

4.3. Vital activities

4.3.1. Photosymbiosis

Photosymbiosis is a well-recognized feature among many modern planktonic foraminiferal species. Recent studies indicate that photosymbiosis in fossil planktonic foraminifera can be recognized by: (1) significantly enriched $\delta^{13}\text{C}$ values due to the preferential uptake of ^{12}C in photosynthesis (Spero and Deniro, 1987; Spero, 1992); (2) a strong positive shift in $\delta^{13}\text{C}$ values with increasing test size due to increased photosymbiotic activity and algal concentration during ontogenetic growth (Houston and Huber, 1998; D'Hondt

Fig. 7. Stable isotope records of analyzed late Cretaceous planktonic foraminifera from DSDP Sites 463 and 577A (equatorial Pacific) and 525A (South Atlantic). Note that *Planoglobulina multicamerata* (Site 577A) and *Heterohelix rajagopalani* (Site 525A) are the most $\delta^{18}\text{O}$ -enriched species, whereas *Pseudoguembelina* spp. are typically the most depleted, suggesting that they were the shallowest dwellers. Keeled globotruncanids mostly display intermediate values. Data in Appendix 1. Key to species: *P. ele* = *P. elegans*; *P. palp* = *P. palpebra*; *P. kem* = *P. kempensis*; *H. lab* = *H. labellosa*; *R. rug* = *R. rugosa*; *G. hav* = *G. havanensis*; *R. rot* = *R. rotundata*; *G. ori* = *G. orientalis*; *P. def* = *P. deformis*; *G. aeg* = *G. aegyptiaca*.

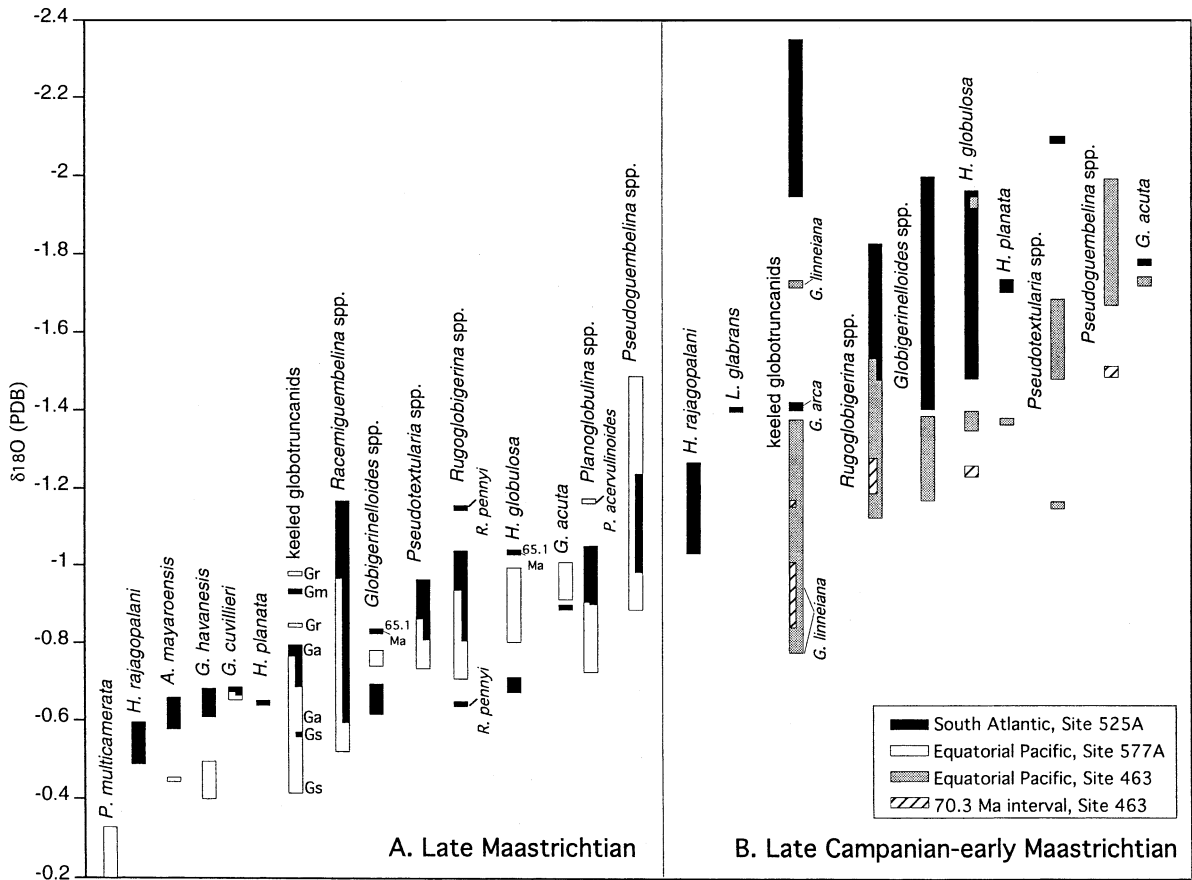


Fig. 8. Oxygen isotope and paleotemperature ranges of major planktonic foraminiferal species and genera in the late Maastrichtian (A), and in the late Campanian-early Maastrichtian (B). Key: Gr, *Globotruncana rosetta*; Gm, *Globotruncana mariei*; Ga, *Globotruncana arca*; Gs, *Globotruncanita stuartiformis*. Maximum intraspecies variation is recorded between the warmest late Campanian (74.3–71.5 Ma) and coldest late Maastrichtian (68.3–65.1 Ma). Note that in both climatic intervals *Pseudoguembelina* species are depleted relative to other species. Also, note the wide isotopic range of *Racemiguembelina* species and the relatively depleted values of keeled globotruncanids in the late Campanian at Site 525A.

and Zachos, 1998; Houston et al., 1999); (3) lighter $\delta^{18}\text{O}$ values compared with coexisting asymbiotic taxa that reflect a high calcification rate in photosymbiotic taxa (Spero, 1992; Norris, 1996); and (4) poor covariance between size-related changes in $\delta^{18}\text{O}$ and $\delta^{13}\text{C}$ values (Houston et al., 1999). Based on these criteria, several late Cretaceous planktonic foraminiferal species can be interpreted as photosymbiotic, including species of the genera *Racemiguembelina*, *Pseudoguembelina*, and *Rugoglobigerina*, as well as *Planoglobulina acervulinoides* and *Heterohelix globulosa* (D'Hondt and Zachos, 1998; Houston and Hu-

ber, 1998; Houston et al., 1999). In addition, it was suggested that *Rugoglobigerina* species represent symbiosis hosting chrysophytes, which generally exhibit a less steep correlation between test size and $\delta^{13}\text{C}$ values, and generally lighter $\delta^{13}\text{C}$ values.

Among the techniques used in previous studies to identify photosymbiotic species, test dissection of single specimens has proved the most successful since it records trends that are unequivocally ontogenetic (Houston et al., 1999). In addition, detection of a positive $\delta^{13}\text{C}$ trend with increasing test size is considered a decisive factor in linking fossils species with photosymbiotic activity be-

cause it rules out other possibilities as the source for enriched $\delta^{13}\text{C}$ values (e.g. affiliation of species to fertile environments or conditions). Nevertheless, the test dissection method requires considerable extra labor (careful removal of individual chambers) and therefore can be applied to only a few designated species. Consequently, photosymbiosis of other species is still unknown. In this report we introduce an alternative approach for preliminary detection of potential photosymbiotic species based on the relative $\delta^{13}\text{C}$ ordering of species within assemblages. This approach is based on the rational that species which consis-

tently display heavier $\delta^{13}\text{C}$ values than species with similar depth affiliations were likely photosymbiotic.

The strongest signals of photosymbiotic activity are recorded by the late Maastrichtian *Racemiguembelina* species (e.g. *R. fructicosa*, *R. powelli*, *R. intermedia*; Plate IV) that exhibit the most enriched $\delta^{13}\text{C}$ values (Figs. 7 and 9). D'Hondt and Arthur (1995) observed the same trend in the North and South Atlantic Sites 390A and 20C, but Pearson et al. (2001) reported a relatively depleted $\delta^{13}\text{C}$ values of *R. fructicosa* in one Maastrichtian sample from Lindi, Tanzania. This dis-

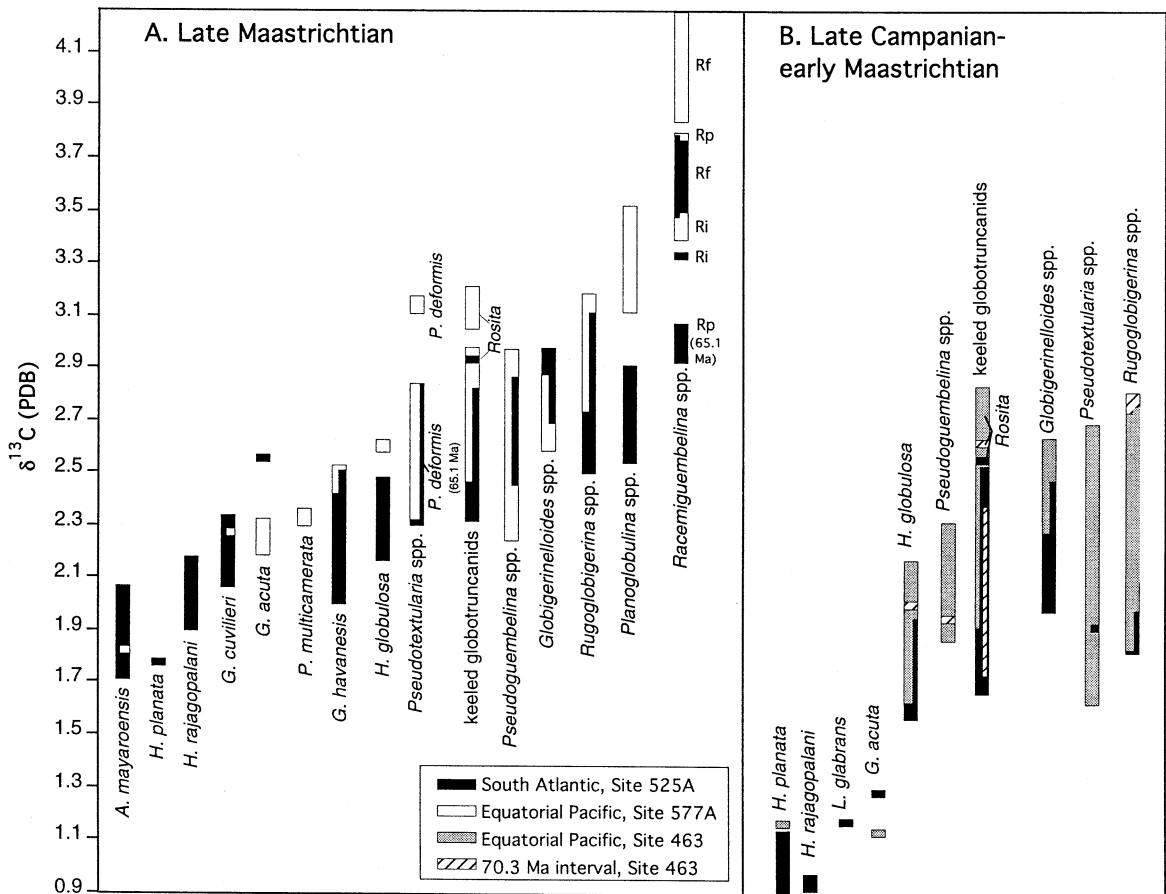


Fig. 9. Carbon isotope ranges of major planktonic foraminiferal species and genera) in the late Maastrichtian (A), and in the late Campanian–early Maastrichtian (B). Key: Rf, *Racemiguembelina fructicosa*; Ri, *Racemiguembelina intermedia*; Rp, *Racemiguembelina powelli*. Note that the isotopic ordering among the *Racemiguembelina* species suggests an increase in photosymbiosis along the development of the morphoseries. The enriched $\delta^{13}\text{C}$ values of the *Rosita* species relative to other keeled globotruncanids implies that they were also photosymbiotic.

crepancy is most likely due to the undeveloped stage and small size of the *R. fructicosa* specimens in the Tanzanian sample (Pearson, pers. commun. 2002). In general, $\delta^{13}\text{C}$ values of *Racemiguembelina* spp. are more depleted in the Atlantic Site 525A than in the Pacific Site 577A (Fig. 9), particularly in the latest Maastrichtian intervals at 65.6 and 65.1 Ma. This may indicate some differences in the intensity of photosymbiotic activity of *Racemiguembelina* between the two localities. A distinctive increase in the $\delta^{13}\text{C}$ trend is recorded among the *Pseudotextularia deformis*–*Racemiguembelina* morpho-series in the late Maastrichtian of the Atlantic and Pacific (Fig. 9) that may signify increased algal density in response to shell size increase.

The $\delta^{13}\text{C}$ data of late Cretaceous planktonic foraminifera in this study are generally consistent with the results of previous studies (e.g. Houston and Huber, 1998; D'Hondt and Zachos, 1998; Houston et al., 1999), and indicate that photosymbiotic activity of the *Racemiguembelina* group was stronger than among *Planoglobulina*, *Pseudoguembelina excolata*, and *Rugoglobigerina* species. Our results also suggest that all morphotypes of the *Rosita* lineage (Plate II) were photosymbiotic (Fig. 9), though additional analyses on individual dissected specimens of *Rosita* are needed to evaluate whether enriched $\delta^{13}\text{C}$ values may reflect a preference for high productivity environments. In addition, our results suggest that photosymbiotic activities varied among localities (e.g. *Racemiguembelina* and *Planoglobulina* and *Rugoglobigerina*) and different climate modes (e.g. *P. excolata*), and may not have existed in certain environments. These observations imply that test dissections of specimens taken from a single sediment sample at a particular locality are not sufficient for characterizing the photosymbiotic activities of these species. Instead, test dissection should be undertaken on specimens selected from various localities and different climate modes.

4.3.2. High respiration

Experiments on extant foraminiferal taxa that quantify the effects of respiration on the concentration of ^{12}C within the foraminiferal shells (Spero et al., 1991, 1993; Spero and Lea, 1996)

suggest that depleted $\delta^{13}\text{C}$ values can result from various metabolic processes. For example, incorporation of metabolic CO_2 during calcification decreases the shell $\delta^{13}\text{C}$ values. At higher respiration rates characteristic of early ontogenetic stages or of small species, a greater percentage of metabolic CO_2 is incorporated into the shell resulting in lighter $\delta^{13}\text{C}$ values. The type of nutrition consumed by foraminifera also has an effect on the shells' $\delta^{13}\text{C}$ signals. Feeding determines the $\delta^{13}\text{C}$ value of the respired CO_2 and, consequently, consumption of different types of food results in different $\delta^{13}\text{C}$ values of respired CO_2 (Spero and Lea, 1996).

Among the late Cretaceous species analyzed for this study, *Abathomphalus mayaroensis*, *Heterohelix planata*, and *Gublerina acuta* (Plates II–III) display exceptionally depleted $\delta^{13}\text{C}$ values that are considerably lighter than expected from their inferred ambient environments (see Section 3.5; Figs. 7 and 9), and therefore may indicate an isotopic contribution of some kind of respiration vital effect mechanism. Depleted $\delta^{13}\text{C}$ values of *A. mayaroensis* are also recorded at the middle and south Atlantic Sites 390A and 690C (D'Hondt and Arthur, 1995). It is interesting that *A. mayaroensis*, *H. planata*, and *G. acuta* do not share morphological features. Moreover, their distinct $\delta^{13}\text{C}$ signals cannot be attributed to ontogenetic development because only adult specimens were collected for this study. It is possible that the exceptionally depleted $\delta^{13}\text{C}$ values of these species signify a feeding source that is particularly enriched with light carbon.

5. Summary and conclusions

- (1) Carbon and oxygen isotope ranking of 56 planktonic foraminiferal species from late Campanian, early, middle and late Maastrichtian intervals permit grouping into deep (sub-thermocline), thermocline, and mixed layer habitats (surface and subsurface). Surface and deep-water habitats were occupied by relatively few species (deep dwellers: *Planoglobulina multicamerata*, *Heterohelix rajagopalani*, *Abathomphalus mayaroensis*, *Globotruncanella havanensis*, *Gublerina cuvillieri*, and

Laeviheterohelix glabrans; surface: *Pseudoguembelina* species).

(2) Most species occupied subsurface depths, though assemblages varied between the thermocline layer and the subsurface mixed layer during cool and warm intervals. During cool climatic intervals, keeled globotruncanids (and perhaps *Globigerinelloides*, and *Racemiguembelina*) occupied the thermocline layer, whereas *Rugoglobigerina*, *Pseudotextularia*, *Planoglobulina* and heterohelicids inhabited the subsurface mixed layer. During the warm climate intervals of the late Campanian, most keeled globotruncanids inhabited the subsurface mixed layer similar to *Rugoglobigerina* in the equatorial Pacific, and even the surface mixed layer in the South Atlantic.

(3) Two distinct types of ‘vital effect’ mechanisms are recognized: (1) photosymbiosis is identified by a repetitive pattern of relatively enriched $\delta^{13}\text{C}$ values, and (2) enrichment of respiration $\delta^{12}\text{C}$ products within the shells, as suggested by distinctly depleted values. Photosymbiotic species include *Racemiguembelina*, *Planoglobulina*, *Pseudoguembelina excolata*, *Rugoglobigerina* and *Rosita*. The coincident appearance of most photosymbiotic species in the late Maastrichtian suggests that this evolutionary development was triggered by oligotrophic conditions associated with increased water-mass stratification.

Acknowledgements

This study benefited from discussions with Chaim Benjamini, Ahuva Almogi-Labin and Paul Pearson. We are grateful to Howard Spero for critical review and many helpful comments. Samples from DSDP Sites 525A, 463 and 577A were provided by the Ocean Drilling Program. This study was supported by BSF grant 98 00425.

Appendix 1

For the stable isotope (\textperthousand) and paleotemperature ($^{\circ}\text{C}$) data of planktonic foraminiferal species in the selected sample intervals of DSDP Sites 525A, 577A and 463 see Table A1

References

- Abramovich, S., Almogi-Labin, A., Benjamini, Ch., 1998. Decline of the Maastrichtian pelagic ecosystem based on planktic foraminiferal assemblage changes: Implications for the terminal Cretaceous crisis. *Geology* 26, 63–66.
- Abramovich, S., Keller, G., Adatte, T., Stinesbeak, W., Hottinger, L., Stüben, D., Berner, Z., Ramanivosa, B., Randriamanantenasoa, A., 2002. Age paleoenvironment of the Maastrichtian-Paleocene of the Mahajanga Basin, Madagascar: A multidisciplinary approach. *Mar. Micropaleontol.* 47, 17–70.
- Barrera, E., 1994. Global environmental changes preceding the Cretaceous-Tertiary boundary: Early-late Maastrichtian transition. *Geology* 22, 877–880.
- Barrera, E., Huber, B.T., 1990. Evolution of Antarctic waters during the Maastrichtian: Foraminifer oxygen and carbon isotope ratios, Leg 113. *Proc. ODP Sci. Results* 119, 813–827.
- Barrera, E., Keller, G., 1990. Foraminiferal stable isotope evidence for gradual decrease of marine productivity and Cretaceous species survivorship in the earliest Danian. *Paleoceanography* 5, 867–890.
- Barrera, E., Keller, G., 1994. Productivity across the Cretaceous/Tertiary boundary in high latitudes. *Geol. Soc. Am. Bull.* 106, 1254–1266.
- Barrera, E., Savin, S.M., 1999. Evolution of late Campanian–Maastrichtian marine climates and oceans. In: Barrera, E., Johnson, C.C. (Eds.), *Evolution of the Cretaceous Ocean–Climate System*. *Geol. Soc. Am. Spec. Pap.* 332, Boulder, CO, pp. 245–282.
- Berggren, W.A., Kent, D.V., Swisher, C.C., Aubry, M.P., 1995. A revised Cenozoic geochronology and chronostratigraphy. *SEPM* 54, 129–213.
- Bleil, U., 1985. The magnetostratigraphy of northwest Pacific sediments, Deep Sea Drilling Project Leg 86. *Init. Rep. DSDP* 86, 441–458.
- Boersma, A., 1981. Cretaceous and early Tertiary foraminifers from Deep Sea Drilling Project Leg 62 Sites in the central Pacific. *Init. Rep. DSDP* 62, 377–397.
- Boersma, A., Shackleton, N.J., 1981. Oxygen and carbon isotope variations and planktonic foraminifer depth habitats, Late Cretaceous to Paleocene, Central Pacific, Deep Sea Drilling Project Sites 463 and 465. *Init. Rep. DSDP* 62, 513–526.
- Bouvier-Soumagnac, Y., Duplessy, J.C., 1985. Carbon and oxygen isotopic composition of planktonic foraminifera from laboratory culture, plankton tows and recent sediments: Implications for the reconstruction of paleoclimate conditions and of the global carbon cycle. *J. Foraminif. Res.* 15, 302–320.
- Caron, M., 1985. Cretaceous planktic foraminifera. In: Bolli, H.M., Saunders, J.B., Perch-Nielsen, K., (Eds.), *Plankton Stratigraphy*. Cambridge Univ. Press, pp. 17–86.
- Chave, A.D., 1984. Lower Paleocene–Upper Cretaceous magnetostratigraphy, Sites 525, 527, 528 and 529, Deep Sea Drilling Project Leg 74. *Init. Rep. DSDP* 74, 525–531.

Table A1

Stable isotope (‰) and paleotemperature (°C) data planktonic foraminiferal species in the selected sample intervals of DSDP Sites 525A, 577A and 463

	DSDP Site 525A								DSDP Site 577A								DSDP Site 463											
	40-2 104–106	40-5 90–92	41-6 89–91	48-3 100–102	50-1 100–102	13-6 42–44	13cc 18–21	10-6 97–100	13-3 97–99	16-6 101–103	20-1 100–102	21-5 64–66	818O Temp.	δ13C	818O Temp.	δ13C	818O Temp.	δ13C	818O Temp.	δ13C	818O Temp.	δ13C	818O Temp.	δ13C	818O Temp.	δ13C		
<i>Abathomphalus mayaroensis</i>	1.88	-0.6615.48	1.70	-0.5815.09	2.06	-0.6015.21																						
<i>Globigerinelloides aspera</i>	2.69	-0.8316.21	2.74	-0.6915.58	2.97	-0.6215.30	2.17	-1.7120.22	1.98	-1.7120.22			1.81 2.58	-0.4514.52 -0.7515.87														
<i>G. subcarinatus</i>																												
<i>G. aff. ultramica</i>							2.47	-2.0021.54	1.96	-1.4118.86			2.51	-1.3818.73														
<i>Globotruncana aegyptiaca</i>							2.41	-2.3423.11					2.86	-0.715.65	2.26	-1.2117.96	1.73	-0.9916.95	2.06	-0.9416.72								
<i>G. arca</i>	2.32	-0.7515.86	2.47	-0.7015.64	2.81	-0.7916.07	1.67	-1.4118.84		2.87	-0.6115.26	2.79	-0.5815.11															
<i>G. bulloides</i>							2.42	-2.2622.73																				
<i>G. diepeblei</i>														2.47	-0.615.20													
<i>G. falostuarti</i>							2.71	-0.6915.60					2.64	-0.5114.81	2.61	-0.5414.93												
<i>G. insignis</i>																												
<i>G. lineata</i>																												
<i>G. mariae</i>	2.58	-0.9416.74																										
<i>G. orientalis</i>																												
<i>G. rosetta</i>																												
<i>G. ventricosa</i>														2.97	-0.4614.57	2.94	-0.5715.06											
<i>Globotruncana angulata</i>													2.72	-0.6715.50	2.59	-0.514.75	2.19	-0.8816.46	1.92	-0.8916.50								
<i>G. calcarea</i>																												
<i>G. stuarti</i>							2.57	-0.8116.14																				
<i>G. stuariformis</i>	2.56	-0.5615.02																										
<i>G. subspissa</i>																												
<i>Globotruncina havaensis</i>	2.01	-0.6715.49					2.50	-0.6115.23							2.52	-0.4114.33	2.42	-0.4914.70										
<i>Gublerina acuta</i>							2.55	-0.9016.55							1.28	-1.7820.54	2.31	-0.9316.69	2.19	-1.1720.00								
<i>G. curvillera</i>	2.32	-0.6415.38	2.06																									
<i>Gansserina gansseri</i>																												
<i>Heterohelix globulosa</i>	2.44	-1.0217.10	2.19	-0.6815.54	2.48	-0.7115.71	1.93	-1.4919.23	1.56	-1.9621.37	2.61	-0.8016.08	2.59	-0.9916.95	1.69	2.20	-1.2318.04	2.11	-1.0117.05									
<i>H. labellata</i>																												
<i>H. planata</i>							1.77	-0.6515.43					0.89	-1.7120.23	1.11	-1.7320.32												
<i>H. punctulata</i>																												
<i>H. rajagopala</i>	2.15	-0.5915.17	1.90	-0.5014.73	2.17	-0.4914.71	0.94	-1.2618.19	0.96	-1.4018.81			1.16															
<i>Laevheterohelix glabrans</i>																												
<i>Planoglobularia cervulinoides</i>	2.89	-1.0417.18	2.71	-0.9116.58																								
<i>P. brauniensis</i>	2.86	-1.0517.24																										
<i>P. caryae</i>	2.54	-1.0117.06	2.53	-0.8416.29																								
<i>P. multicamerata</i>																												
<i>Pseudoumbelina costulata</i>							2.56	-1.0517.24																				
<i>P. exoculata</i>																												
<i>P. hawaiiensis</i>	2.79	-1.1117.47	2.70	-1.1417.62																								
<i>P. kempensis</i>																												
<i>P. palpebra</i>	2.95	-1.2318.02				2.62	-0.9916.94																					
<i>Pseudotextularia deformis</i>	2.53	-0.8116.16	2.69	-0.8216.18																								
<i>P. elegans</i>	2.62	-0.9616.83	2.42	-0.9016.54	2.83	-0.8716.43	1.99	-2.1022.01																				
<i>Racemicumbella fructicosa</i>					3.48	-0.6015.21	3.77	-1.0817.36																				
<i>R. intermedia</i>							3.33	-1.0617.27																				
<i>R. powelli</i>	2.92	-0.9116.59	3.06	-1.1717.77	3.31	-0.7515.87																						
<i>Rosita fornicate</i>																												
<i>R. patelliformis</i>																												
<i>R. plicata</i>																												
<i>R. plummerae</i>																												
<i>R. walfishensis</i>		3.00	-0.7916.06																									
<i>Rugoglobularia hexacamerata</i>							3.17	-1.0617.27																				
<i>R. macrocephalla</i>																												
<i>R. milamensis</i>																												
<i>R. pennyi</i>	2.58	-1.1517.67			2.65	-0.6415.36	1.97	-1.8220.74	1.82	-1.4819.18																		
<i>R. rugosa</i>	2.63	-0.9316.67	2.62	-0.8116.14	2.76	-0.8516.32	1.99	-1.7620.43	1.89	-1.5419.45	2.91	-0.8516.32	2.87	-0.7215.74	2.32	-1.1517.68	2.76	-1.2017.91	2.33	-1.1217.53	2.75	-1.3118.40	2.51	-1.1517.68				
<i>R. rotundata</i>																												
<i>R. scotti</i>																												
<i>Abathomphalus mayaroensis</i>	1.88	-0.6615.48	1.70	-0.5815.09	2.06	-0.6015.21		-1.7120.22	1.98	-1.7120.22																		
<i>Globigerinelloides aspera</i>	2.69	-0.8316.21	2.74	-0.6915.58	2.97	-0.6215.30	2.17	-1.7120.22	1.98	-1.7120.22																		
<i>G. subcarinatus</i>																												
<i>G. aff. ultramica</i>															2.47	-2.0021.54	1.96	-1.4118.86										
<i>Globotruncana aegyptiaca</i>															2.41	-2.3423.11												
<i>G. arca</i>	2.32	-0.7515.86	2.47	-0.7015.64	2.81	-0.7916.07	1.67	-1.4118.84		2.87	-0.6115.26	2.79	-0.5815.11															
<i>G. bulloides</i>															2.42	-2.2622.73												
<i>G. diepeblei</i>																												
<i>G. falostuarti</i>																												
<i>G. insignis</i>																												

Table A1 (*Continued*).

- D'Hondt, S., Lindinger, M., 1994. A stable isotope record of the Maastrichtian ocean-climate system: South Atlantic DSDP Site 528. *Palaeogeogr. Palaeoclimatol. Palaeoecol.* 112, 363–378.
- D'Hondt, S., Arthur, M.A., 1995. Interspecies variation in stable isotopic signals of Maastrichtian planktonic foraminifera. *Paleoceanography* 10, 123–135.
- D'Hondt, S., Arthur, M.A., 1996. Late Cretaceous oceans and the cool tropic paradox. *Science* 271, 1838–1841.
- D'Hondt, S., Zachos, J., 1998. Cretaceous foraminifera and the evolutionary history of planktic photosymbiosis. *Paleobiology* 24, 512–523.
- Douglas, R.G., Savin, S.M., 1978. Oxygen isotopic evidence for depth stratification of Tertiary and Cretaceous planktic foraminifera. *Mar. Micropaleontol.* 3, 175–196.
- Emiliani, C., 1971. Depth habitats of growth stages of pelagic foraminifera. *Science* 173, 1122–1124.
- Erez, J., Luz, B., 1983. Experimental paleotemperatures equation for planktonic foraminifera. *Geochim. Cosmochim. Acta* 47, 1025–1031.
- Fairbanks, R.G., Sverdrup, M., Free, R., Wiebe, P.H., Bé, A.W.H., 1982. Vertical distribution and isotopic fractionation of living planktonic foraminifera from the Panama Basin. *Nature* 298, 841–844.
- Houston, R.M., Huber, B.T., 1998. Evidence of photosymbiosis in fossil taxa? Ontogenetic stable isotope trends in some late Cretaceous planktonic foraminifera. *Mar. Micropaleontol.* 34, 29–46.
- Houston, R.M., Huber, B.T., Spero, H.J., 1999. Size-related isotopic trends in some Maastrichtian planktic foraminifera: Methodological comparisons, intraspecific variability and evidence for photosymbiosis. *Mar. Micropaleontol.* 36, 169–188.
- Keller, G., 1996. The Cretaceous-Tertiary mass extinction in planktonic foraminifera: Biotic constraints for catastrophe theories. In: MacLeod, N., Keller, G., (Eds.), *Cretaceous-Tertiary Mass Extinction Biotic and Environmental Changes*. Norton, New York, pp. 49–84.
- Keller, G., 2001. The end-Cretaceous mass extinction in the marine realm: Year 2000 assessment. *Planet. Space Sci.* 49, 817–830.
- Keller, G., Adatte, T., Stinnesbeck, W., Luciani, V., Karoui, N., Zaghibib-Turki, D., 2002. Paleoecogeography of the Cretaceous-Tertiary mass extinction in planktic foraminifera. *Palaeogeogr. Palaeoclimatol. Palaeoecol.* 178, 257–298.
- Li, L., Keller, G., 1998a. Maastrichtian climate, productivity and faunal turnovers in planktic foraminifera in South Atlantic DSDP Sites 525A and 21. *Mar. Micropaleontol.* 33, 55–86.
- Li, L., Keller, G., 1998b. Abrupt deep-sea warming at the end of the Cretaceous. *Geology* 26, 995–998.
- Li, L., Keller, G., 1998c. Diversification and extinction in Campanian-Maastrichtian planktic foraminifera of north-western Tunisia. *Eclogae geol. Helv.* 91, 75–102.
- Li, L., Keller, G., 1999. Variability in Late Cretaceous climate and deep water: Evidence from stable isotopes. *Mar. Geol.* 161, 171–190.
- Lohmann, G.P., 1995. A model for variation in the chemistry of planktonic foraminifera due to secondary calcification and selective dissolution. *Paleoceanography* 10, 445–458.
- Malmgren, B.A., 1991. Biogeographic patterns in terminal Cretaceous planktonic foraminifera from Tethyan and warm Transitional waters. *Mar. Micropaleontol.* 18, 73–99.
- Masters, B.A., 1977. Mesozoic planktonic foraminifera. In: Ramsay, A.T.S. (Ed.), *Oceanic Micropaleontology*. Academic Press, London, pp. 301–731.
- Nederbragt, A.J., 1991. Late Cretaceous biostratigraphy and development of *Heterohelicidea* (planktic foraminifera). *Micropaleontology* 44, 385–412.
- Nederbragt, A.J., 1998. Quantitative biogeographic of late Maastrichtian planktic foraminifera. *Micropaleontology* 44, 385–412.
- Norris, R.D., 1996. Symbiosis as an evolutionary innovation in the radiation of Paleocene planktic foraminifera. *Paleobiology* 22, 461–480.
- Pearson, P.N., Ditchfield, P.W., Singano, J., Harcourt-Brown, K.G., Nicholas, C.J., Olsson, R.K., Shackleton, N.J., Hall, M.A., 2001. Warm tropical sea surface temperatures in the Late Cretaceous and Eocene epochs. *Nature* 413, 481–487.
- Robaszynski, F., Caron, M., Gonzales Donoso, J.M., Wonders, A.A.H., 1983. Atlas of Late Cretaceous Globotruncanids. *Rev. Micropaleontol.* 26, 145–305.
- Schrag, D.P., 1999. Effect of diagenesis on the isotopic record of late Paleogene tropical sea surface temperatures. *Chem. Geol.* 161, 215–224.
- Schrag, D.P., DePaolo, D.J., Richter, F.M., 1995. Reconstructing past sea surface temperatures from oxygen isotope measurements of bulk carbonate. *Geochim. Cosmochim. Acta* 59, 2265–2278.
- Schweitzer, P.N., 1993. Modern Average Global Sea-Surface Temperature. Geological Survey Digital Data Series, DDS-10.
- Shackleton, N.J., Kennett, J.P., 1975. Paleotemperature history of the Cenozoic and the initial of Antarctic glaciation: Oxygen and carbon isotope analyses in Deep Sea Drilling Project Sites 277, 279, and 181. *Init. Rep. DSDP* 29, 599–612.
- Smith, C.C., Pessagno, E.A.Jr., 1983. Planktonic foraminifera and stratigraphy of Corsicana Formation (Maastrichtian) north-central Texas. Contribution from the Cushman Foundation. *Foraminif. Res. Spec. Publ.* 12, 5–66.
- Spero, H.J., 1992. Do planktic foraminifera accurately record shifts in the carbon isotopic composition of seawater ΣCO_2 ? *Mar. Micropaleontol.* 19, 275–285.
- Spero, H.J., Deniro, M.J., 1987. The influence of symbiont photosynthesis on the $\delta^{18}\text{O}$ and $\delta^{13}\text{C}$ values of planktonic foraminiferal shell calcite. *Symbiosis* 4, 213–228.
- Spero, H.J., Lea, D.W., 1996. Experimental determination of stable isotope variability in *Globigerina bulloides*: Implications for paleoceanographic reconstructions. *Mar. Micropaleontol.* 28, 231–246.
- Spero, H.J., Lerche, I., Williams, D.F., 1991. Opening the

- carbon isotope ‘vital effect’ black box, 2. Quantitative model for interpreting foraminiferal carbon isotope data. *Paleoceanography* 6, 639–655.
- Spero, H.J., Anderson, D.J., Sorgeloos, P., 1993. Carbon and nitrogen isotopic composition of different strains of *Artemia*. *Sp. Int. J. Salt Lake Res.* 2, 133–139.
- Stott, L.D., Kennett, J.P., 1990. The paleoceanographic and climatic signature of the Cretaceous/Paleogene boundary in the Antarctic: Stable isotopic results from ODP Leg 113. *Proc. ODP. Sci. Results* 113, 829–848.
- Stüben, D., Kramar, U., Berner Z., Leesson M.A., Meudt, M., Keller, G., Abramovich, S., Adatte, T., Hambach, Stinnesbeck, W., in press. Late Maastrichtian paleoclimatic and paleoceanographic changes inferred from Ca/Sr and stable isotopes. *Palaeogeogr. Palaeoclimatol. Palaeoecol.*
- Wu, G., Berger, W.H., 1990. Planktic foraminifera: Differential dissolution and the Quaternary stable isotope record in the west equatorial Pacific. *Paleoceanography* 4, 181–198.
- Zachos, J.C., Arthur, M.A., Thunell, R.C., Williams, D.F., Tappa, E.J., 1985. Stable isotope and trace element geochemistry of carbonate sediments across the Cretaceous/Tertiary boundary at Deep Sea Drilling Project Hole 577. *Init. Rep. DSDP* 86, 513–532.
- Zachos, J.C., Arthur, M.A., Dean, W.E., 1989. Geochemical evidence for suppression of pelagic marine productivity at the Cretaceous/Tertiary boundary. *Nature* 337, 61–64.